Reexamination of Tropical Cyclone Wind-Pressure Relationships

John A. Knaff
CIRA
Colorado State University
Fort Collins, CO

Raymond M. Zehr
NOAA/NESDIS
Fort Collins, CO

Revised for

Weather and Forecasting

April 10, 2006

Corresponding Author: John Knaff, CIRA, Colorado State University, Fort Collins, CO 80523-1375, 970 491-8881, knaff@cira.colostate.edu

Abstract

Tropical cyclone wind-pressure relationships are reexamined using 15 years of minimum sea level pressure estimates, numerical analysis fields and best track intensities. Minimum sea level pressure is estimated from aircraft reconnaissance or measured from dropwindsonds and maximum wind speeds are interpolated from best track maximum 1-minute wind speed estimates. The aircraft data were collected primarily in the Atlantic but also include eastern and central North Pacific cases. Global numerical analyses were used to estimate tropical cyclone size and environmental pressure associated with each observation.

Using this dataset (N=3801) the influences of latitude, tropical cyclone size, environmental pressure, and intensification trend on the tropical cyclone wind-pressure relationships were examined. Findings suggest that latitude, size and environmental pressure, which all can be quantified in an operational and post analysis setting, are related to predictable changes in the wind-pressure relationships. These factors can be combined into equations that estimate winds given pressure and estimate pressure given winds with greater accuracy than current methodologies. In independent testing during the 2005 hurricane season (N=524), these new wind-pressure relationships resulted in mean absolute errors of 5.3 hPa and 6.2 kt compared to 7.7 hPa and 9.0 kt that resulted from using the standard Atlantic Dvorak wind-pressure relationship.

These new wind-pressure relationships are then used to evaluate several operational wind-pressure relationships. These intercomparisons have led to several recommendations for operational tropical cyclone centers and those interested in reanalyzing past tropical cyclone events.

1. Introduction

Possibly the most accurate and reliable measure of tropical cyclone (TC) intensity is the minimum sea level pressure (MSLP) either estimated from aircraft reconnaissance flight level or obtained via direct observation (surface or dropwindsonde). However, the destructive potential of TCs is better related to the maximum wind speed at or near the surface. For this reason, TC forecasts and advisories as well as climatological records are most useful when they describe TC intensity in terms of maximum surface wind speed (10-m level,1-minute sustained, 10-minute average, etc…) – a difficult quantity to measure. This reality has lead to the development of relationships between the MSLP and maximum surface wind speed, which are used both operationally and in post analysis of individual TC events. While these "wind-pressure relationships" attempt to describe the mean relationship between the MSLP and maximum wind, the actual relationship is a function of several factors related to TC environment and structure that vary from case to case. As a result, there is considerable scatter about any given wind-pressure relationship (WPR).

Since TCs are well approximated by the gradient wind balance (Willoughby 1990, Willoughby and Rahn (2004)), one need only examine the cylindrical form of gradient wind equation in azimuthal mean and integral form (Eq. 1) to better understand what factors determine the MSLP in a TC (Hess, 1959).

$$MSLP = P_{env} - \int_{r=0}^{r_{env}} \rho \left(\frac{V_t^2}{r} + fV_t \right) dr \qquad (1)$$

Two obvious factors are size, which is given by the radius of the environmental pressure (r_{env}) and environmental pressure (P_{env}). A more subtle factor is the integral of

$\rho\left(\frac{V_t^2}{r} + fV_t\right)$, where V_t is the tangential wind ρ is density and f is the Coriolis force ($f=2\Omega\sin(\phi)$, where ϕ is latitude). This integral term accounts for a number of factors (radius of maximum winds, secondary wind maxima etc.) that are difficult to accurately measure operationally and climatologically, particularly in the absence of aircraft reconnaissance data. The authors concede that in some circumstances the radius of maximum winds can be accurately estimated using satellite techniques and quite often when aircraft reconnaissance is available. Nonetheless any variation in the radial profile of tangential wind will change the MSLP and in turn may greatly influence how MSLP is related to the maximum surface wind.

In a modern operational setting with satellite imagery and quality global analyses, five basic factors that affect the WPR can always be estimated in operations; namely size, latitude, environmental pressure, storm motion and intensification trend. The first two, size and latitude determine the potential magnitude of the integral in Eq. 1. Storm motion has been shown to slightly influence the maximum surface wind speeds associated with TCs resulting in slightly greater intensities for faster moving storms if all other factors are held constant (Schwerdt et al. 1979). The intensification trend has also been shown to be an important factor for the slope of the WPR (Koba et al. 1990). This is likely due to the shape of the radial profiles of the tangential wind being a function of intensification trend.

In the situation when aircraft reconnaissance is available, there less of a need for WPRs as the flight-level winds, a proxy for surface winds, and MSLP are measured independently. Surface winds are routinely estimated from flight level (e.g., as described

in Franklin et al. 2003), though there is still uncertainty in such estimates. Thus, WPRs can provide additional independent information when other techniques (i.e., satellite-based intensity estimates) have estimated either the MSLP or maximum surface wind speeds. This application however, may be more important during the post-operational reanalysis of storm intensity.

Historically, WPRs have been derived primarily by making use of two methods. The first is to assume cyclostrophic balance (Eq. 2)

$$V_t^2 = \frac{r}{\rho}\frac{\partial p}{\partial r}, \qquad (2)$$

where r is the radius p is pressure, and ρ density. In application, a loose approximation of cyclostrophic balance (Eq. 3)

$$V_{\max} = C\left(P_{ref} - P_c\right)^n \qquad (3)$$

is most often applied, where P_{ref} is a reference Pressure, P_c is the MSLP, C is an empirical constant and n is an empirical exponent; noting that n=0.5 represents cyclostophic balance. In this methodology, historical data is used to find the best fit to parameters C and n. However, as Landsea et al. (2004) points out, since the numbers of weaker cases often outnumber the stronger cases, one should bin the cases by intensity before finding the best fit. The second common methodology makes uses of maximum wind speed or MSLP composites. However, the development of WPRs in the past has been most challenged by the relatively few cases available for their development rather than what methodology is used to fit the data.

Five different WPRs have been used at the operational TC centers throughout the world. They are:

1. Atkinson and Holliday (1977;1975) used at Regional Specialized Meteorological Centre (RSMC) La Reunion, RSMC Fiji, the Perth tropical cyclone centre, and at the Joint Typhoon Warning Center,
2. Koba et al. (1990) used at the RSMC Tokyo,
3. Love and Murphy (1985) used in the Australian Northern Territory tropical cyclone warning centre in Darwin,
4. a method attributed to Crane used at the Brisbane tropical cyclone warning centre, and
5. Dvorak (1975) (i.e., the Atlantic part of the table) is used for the Atlantic and East Pacific at NHC/TPC and Central Pacific at the Central Pacific Hurricane Center.

These relationships are shown in Fig. 1a in terms of $\Delta P=(MSLP-P_{env})$. Also shown in Fig. 1b are the four WPRs used by Landsea et al. (2004) for the Atlantic best track reanalysis (1850-1910) in terms of $\Delta P=(MSLP-1013)$. All of the operational WPRs, except Atkinson and Holliday (1977) (A&H), were compiled using composite methods, most used relatively limited datasets, and all were developed more than 15 years ago. For a more comprehensive review of the history of WPRs and the individual wind vs. pressure methodologies, reading Harper (2002) is recommended. However, two historical points from Harper (2002) are important to the remainder of this paper. First, unlike the development of other WPRs and despite the laborious task of assembling the A&H dataset, A&H did not bin their data by intensity before creating a best fit. Secondly, the Dvorak (1975) WPRs are derived from primarily from western Pacific

MSLP measurements and are identical save for the offset of 6 hPa to account for the lower environmental pressure in the western North Pacific.

Given the curves in Fig 1, it is only natural to question the relative accuracy of these methods and ask whether or not one can develop better techniques with a greater number of cases and with more recently collected datasets. One consideration is that more recent best track data that takes into account near surface wind measurements from GPS dropwindsondes (circa 1997) as well as flight-level to surface wind reduction factors developed using GPS dropwindsonde information (Franklin et al. 2003), which have been used in operations since ~ 2002. However, it is worth noting that the flight-level to surface wind reduction factors have varied somewhat during the period of analysis. Also available are quality reanalyses of atmospheric conditions (Kalney et al 1998), which can be used to estimate TC size and environmental conditions. It is also now know that TCs are closely approximated by gradient wind balance (Willoughby 1990) and that cyclostrophic balance is a less accurate balance approximation.

In addition to the operational considerations, the estimates of WPRs have become the basis of some of the TC intensity climatology. For instance in the past it was routine to estimate the MSLP from aircraft and then assign the winds according to that pressure. Any errors or biases in these past estimates remain in the current best track intensity estimates. Such errors and biases as well as others resulting from changes in operational procedures have become particularly important with recent publications showing dramatic upward trends in the intensities of global TCs (i.e., Emanuel 2005; Webster et al. 2005).

With the above factors in mind, the aim of this paper is to better understand the scatter between MSLP and TC maximum wind speeds, use this knowledge to evaluate operational WPRs and to make recommendations based on those assessments. To this end, composites of the WPR stratified by size, latitude and intensity trend are created. It is important to note that since the systematic differences between TC basins (latitude, size, and P_{env}) are explicitly accounted for in this methodology, the resulting WPRs are applicable to any TC. The pressure observations come from aircraft data and the maximum wind speeds are interpolated to the time of the pressure observation from the best track. A unified regression approach will be developed from the composites. Finally, using this unified approach, the WPRs used in operations and for best track and climatological reanalysis will be examined, and recommendations made.

2. Datasets

This is a 15-year study (1989-2004) that makes use of three separate datasets; aircraft MSLP estimates or dropwindsonde measurements in the eye, TC best tracks, and NCEP reanalysis and analysis fields. Aircraft intensity fixes are maintained in a digital database that is part of the Automated Tropical Cyclone Forecast (ATCF) system (Sampson and Schrader 2000). Each aircraft intensity fix has a time (nearest minute), location (nearest 10^{th} of a degree), and intensity MSLP (nearest hPa) associated with it. These fixes are the foundation for this study and are the points in time and space by which environmental pressure and cyclone size are estimated. Aircraft fixes are mostly located in the Atlantic TC basin, but there are a few (N=268) storm fixes available in the central and eastern North Pacific. Fixes within 30 km of land are not used in this study to

limit the effects of landfall induced intensity change. Figure 2 shows the location of the points (n=3801) used in this study. Tropical cyclone maximum wind speeds in the operational advisories and historical TC databases are given to the nearest 5 knots (kt), where 1 kt = 0.52 m/s. For this reason, the non-standard unit of kt is used for wind speeds throughout this paper. For the remainder of this paper V_{max} refers to the 1-minute sustained 10-meter wind speed in units of kt, as is the convention at the NHC. To better compare western North Pacific WPRs, similar fixes containing the MSLP data collected by aircraft reconnaissance are utilized (1966-1987).

Tropical cyclone best tracks are created following the TC season and include the best estimate of location and intensity every six hours (Jarvinen et al. 1984). The best tracks are archived in an ATCF database and are available from the National Hurricane Center. Maximum wind speeds and storm translation speeds are interpolated to the aircraft fix time from 6-hourly values in the best track files. Maximum wind 12 hours prior to the aircraft fix time is also calculated in the same manner. The 12-h intensity trend is then easily calculated. Figure 3 is a plot of the wind speeds reported in the best tracks versus the maximum 10-second wind reported at flight level within three hours of the best track time in the Air Force aircraft reconnaissance data 1995-2004, which were observed using a common flight pattern at standardized heights. The high correlation ($R^2 = 0.90$) between these datasets indicate that best track estimates of maximum winds are influenced by flight level wind values in a systematic manner. Best track data from the western North Pacific, maintained by the JTWC, are used in the evaluation operational WPRs in that region (JTWC, cited 2006).

The translation speed of a storm has a small influence on maximum surface winds in a TC, which it is desirable to remove for this study. To remove this influence of storm motion, a storm relative maximum surface wind speed (V_{srm}) is estimated by $V_{srm} \approx V_{max}$-$1.5c^{0.63}$ as suggested by Schwerdt et al. (1979). This approximation assumes that the maximum winds are to the right of the TC motion in the Northern Hemisphere, which is the case with flight level winds (Mueller et al. 2006) that are often used in operations to estimate V_{max}. The maximum surface wind's location is still a point of scientific debate (e.g., Kepert 2001; Kepert and Wang 2001).

Six-hourly NCEP analyses are used to estimate the TC size and environmental sea level pressure conditions for each aircraft fix. Operational analyses are used for years 2001 to present and NCEP reanalysis fields are used prior to that time.

Since it is the gradient of the pressure that is best related to the wind field, the environmental pressure in which a TC is embedded should be accounted for in any study of TC WPRs. An environmental pressure for each fix is estimated by calculating the azimuthal mean pressure in an 800 to 1000 km annulus surrounding the cyclone center at each adjacent reanalysis time. To make the calculation the MSLP is interpolated to a finer grid (10 km). These interpolated values are then averaged if they fall within the 800 to 1000 km annulus. The final estimate is determined by interpolating the 6-hourly estimates to the time of the aircraft fix. Using this estimate of environmental pressure (P_{env}) a pressure deficit (ΔP) is estimated by subtracting P_{env} from the MSLP provided by the aircraft fix.

In an operational setting, TC size is described by the radial extent of gale force winds or the radius of the outer most closed isobar. Both quantities are estimated by the

warning agency, which for most cases in this study is NHC. The size can also be evaluated by the wind fields in the reanalysis data. Ideally, the size would be quantified according to the radius of zero tangential winds, however this quantity is very difficult to determine. Fortunately, the average tangential winds calculated from the NCEP analyses in the annulus of 400-600 km (V_{500}), calculated in the same manner as P_{env}, correlates with TC size. The tangential winds in this annulus are not only resolved by the global numerical analyses, but often correspond with the radial extent of the cirrus canopy and (Kossin 2002; Knaff et al. 2003). Figure 4 shows the relationship ($R^2 = 0.25$) between V_{500} and the average radius of 34-kt winds reported in the NHC advisories (1995-2004). Additionally it is recognized that TC size is also influenced by differences in intensity and latitude (see Eq. 1). In order to evaluate a range of tropic cyclone sizes for differing intensities and locations, a normalized size parameter is developed.

To remove the influence of TC intensity and latitude from the size estimate, the V_{500} is then divided by the value by the climatological tangential wind 500 km from the center (V_{500c}), which is estimated using a modified rankine vortex (Eq. 4),

$$(4)\ V_{500c} = V_{\max}\left[\frac{R_{\max}}{500}\right]^{x},$$

where x, the shape factor (Eq 5), and R_{max}, the radius of maximum winds in km (Eq. 6), are functions of latitude(ϕ) in degrees and intensity (V_{max}) in kt.

$$(5)\ x = 0.1147 + 0.0055V_{\max} - 0.001(\phi - 25)$$

$$(6)\ R_{\max} = 66.785 - 0.09102V_{\max} + 1.0619(\phi - 25)$$

Coefficients for this modified Rankine vortex model are derived from the operational Atlantic wind radii Climatology and Persistence model described in Gross et al. (2004), and Knaff et al. (2006). These equations are valid for $V_{max} \geq 15$ kt.

For each aircraft fix a value of V_{500} is estimated by interpolating values calculated at adjacent analysis times to the time associated with the fix. The value of V_{500} is then normalized by dividing this value by V_{500c}.

In summary, aircraft fixes for the period (1989-2004) collected in the Atlantic and central and eastern North Pacific provide a date/time, location and MSLP associated with various TCs. Aircraft fixes within 30 km of land are excluded from the dataset. Using the times and locations of the remaining fixes, the best track maximum winds, 12-h trends and intensities and 12-hour motion are interpolated to the time of each fix. The effects of storm motion are removed then from the intensity estimate to form a storm relative maximum surface wind, V_{srm}. Similarly, NCEP analyses are used to estimate the environmental sea level pressure 800 – 1000 km (P_{env}) and the average tangential winds at 400 - 600 km (V_{500}) associated with each fix. The influence of the P_{env} is then subtracted from each MSLP fix to form a pressure deficit (ΔP). The estimate of V_{500} is divided by a climatological value (Eq. 4-6) to form a normalized TC size parameter, which is used to estimate and account for variations in TC size. Combining this information results in 3801 cases with estimates of time, location, MSLP, P_{env}, ΔP, V_{max}, V_{srm}, 12-hour trends of V_{max}, 12-hour motion, and TC size. These parameters are used in the following sections to reexamine TC WPRs.

3. Methodology

There are five basic factors that affect the WPR considered in this study that can be both estimated with current datasets and in an operational setting. These include environmental pressure, storm motion, latitude, storm size, and intensification trend. In the following section each of these factors will be discussed. Other factors, associated with the radial distribution of tangential winds, particularly variations in the radius of maximum wind (RMW), are not considered.

Statistics associated with each composite and the whole dataset are shown in Table 1. Individual composites are created by binning V_{srm} every 2.5 kts for V_{srm} values less than or equal to 70 kt and every 5 kt for V_{srm} values above 70 kt. In the cases where there are less than 10 individual cases in a bin those cases are combined with the next ascending bin (s) until at least 10 cases are utilized in each average. Detailed results of these stratifications will be discussed in the subsections in Section 4.

Using the composites based upon latitude, size and intensity trend, which are binned by intensity, regression equations are developed for each composite using predictors that closely approximate the likely best fit associated with gradient wind balance (i.e., $\Delta P \approx aV_{srm}^2 + bV_{srm} + C$). The deviation from historical practice is justified by our current knowledge that TCs are well approximated by gradient balance rather than cyclostrphic balance. These equations then will be used to estimate the value of ΔP for each Dvorak CI number given in Appendix B.

In addition, the composite averages of each of the individual composites are used to create one unifying regression equation that can be used to predict ΔP as a function of

V_{max}, latitude, size and intensity trend. Likewise regression equations will be developed for V_{max} (i.e., , $V_{srm}(\Delta P) = a\Delta P + b\sqrt{|\Delta P|} + C$, and $V_{max} = V_{srm} + 1.5c^{0.63}$, where c is storm motion), but just for those stratifications that would be used for climatological reanalysis. These unified approaches will be discussed in Section 5. These unified regression equations will be compared with techniques used both operationally throughout the world and for best track reanalysis activities in Section 6.

4. Factors influencing pressure wind relationships

a. Environmental pressure

For the 3801 case dataset, the mean value of P_{env} is 1014.3 hPa, the standard deviation is 2.5 hPa, the maximum is 1025.1 hPa and the minimum is 1004.5 hPa. Figure 5, which shows MSLP vs V_{max} and ΔP vs. V_{max} illustrates the effect of using ΔP instead of MSLP when developing WPRs. There is a very small reduction (i.e., 0.3%) in the variance explained by a linear fit of ΔP compared to MSLP, and the resulting scatter in Fig 5b is still substantial.

b. Storm motion

Storms that translate at faster speeds have been shown to have slightly larger maximum surface (Schwerdt et al. 1979) and flight level winds (Mueller et al. 2006). Storm motion in this sample had a mean value of 9.6 kt with a standard deviation of 4.6 kt and ranged from 0 kt to 34.8 kt. Figure 6 shows the scatter diagram of ΔP vs V_{max} and ΔP vs V_{srm}. the effect of removing this factor on the WPR. Again as was the case with removing the

effects of P_{env}, removing the influence of storm motion has a relatively small effect on the reduction of the scatter, increasing the variance explained by about 0.2%.

c. Latitude

As latitude increase, the Coriolis force also increases requiring lesser tangential wind to balance the pressure gradient force. As a result higher latitude storms have lower pressures given the same radial wind profile. To explore the influence of latitude in our dataset composites are constructed. The average latitude of the whole sample is 23.7^{o}N with a standard deviation of 6.4^{o}. Latitude-based composites are constructed from fixes for regions equatorward of 20^{o} latitude, between 20^{o} and 30^{o} latitude, and greater than 30^{o} latitude. This resulted in 1226, 1970, and 659 cases, respectively. The mean quantities of the individual composites are shown in Table 1.

The composite results of the latitudinal stratification (Fig. 7) show that the ΔP vs. V_{srm} relationship is clearly a function of latitude. The differences seem fairly systematic for V_{srm} values greater than 45 kt. In this intensity range there is approximately 5 hPa decrease for every 10 degrees of latitude. These composites confirm that for a given V_{srm} a low latitude storm will on average have higher values of ΔP.

d. Size

Following gradient wind balance, large TCs have smaller V_{max} for a given ΔP because the pressure gradient is distributed over a larger radial distance. Figure 8 shows the relationship between the size parameter (i.e., V_{500} / V_{500c}) and the average radius of 34-kt winds from the advisories. The size parameter explains 40% of the variance of the average radius of 34-k winds (the sample mean radius of 34-kt winds is 110 nm). As test to see if the size parameter was really indicating size we examined the tails of the

distribution for storms with V_{max} > 100kt. The largest storms with these intensities were all from the Atlantic; Isabel (2003), Floyd (1999), Luis (1995), Gert (1995) and Mitch (1999) – all notably large storms. The smallest storms were Charlie (2004), and Andrew (1992) from the Atlantic, John (1994, south of Hawaii) and Olivia (1994) from the East Pacific, and Iniki (1992) from the central Pacific, all notably small storms. Examining the seasonal summaries and other information available about these storms, it appears that the size parameter is providing a good estimate of TC size. Further evidence is presented in the composite means.

Based on this size parameter, three composites are created containing small, average, and large storms. The distribution of this TC size measure is nearly normal with a mean value of 0.49 and a standard deviation of 0.22. The composites consist of those cases less than one standard deviation from the mean (small), between +1 and -1 standard deviations from the mean (average) and those cases with sizes greater than 1 standard deviation from the mean (large) resulting in 595, 2562, and 644 cases, respectively. Further size stratification (e.g., those used in Merrill 1984) was not attempted as the number of large TC cases became too small. Again, mean quantities associated with each composite are shown in Table 1.

The WPRs resulting from the composite averages are shown in Figure 9. Interestingly, the differences between small TC and average-sized TC composites are rather small, but for the large storms, 16.9% of the sample, ΔP tended to be significantly lower than storms with similar V_{srm}. In Fig. 9, there appears to be a slight discontinuity in the large composite cases occurring in the intensity range 85 to 120 kt that requires further explanation. This was examined and is related to the mean latitude of the

composite averages stratified by intensity. As the intensity increased, the mean latitude decreased from ~28^{o} at 85 kt to ~20^{o} at 125 kt.

e. Intensity trend

Koba et al. (1990), using surface MSLP and satellite wind estimates gathered in the western North Pacific, found that the WPR was also a function of intensity trend. The steady and weakening (intensifying) storms tended to have lower (higher) pressures at intensities below 65 kt strength (i.e., Dvorak T-number ~ 5.5) and higher (lower) pressures above this threshold. These trends may be the result of the TC lifecycle and typical structural differences (vortex size and radius of maximum winds) between developing and decaying TCs (i.e., those discussed in Weatherford and Gray (1988)). Composites of steady and weakening storms are compared with those that are weakening, repeating the analysis of Koba et al. (1990). Mean statistics associated with these composites are shown in Table 1.

Composite averages based on intensity trends are shown in Fig. 10. These data confirm the results reported in Koba et al. (1990) that showed that weakening/steady and intensifying storms have different WPRs. The shapes of these curves suggest that the intensity trend of a given storm is an important factor to determining the WPR.

Using independent data, the differences found by Koba et al. (1990) were confirmed here. Findings show that weakening/steady (intensifying) storms have a tendency to have lower (higher) pressures below approximately intensities of ~40-65 kt and higher (lower) pressures at intensities greater than ~40-65 kt. However, examining the composite results with respect to trend also shows that the intensifying storms are smaller and at lower latitude than the weakening storms in the same ranges of maximum

wind speed in which the WPR has the greatest differences. Figure 11 shows the average size and average latitude versus the storm relative maximum wind for the intensifying and steady/weakening composites. Furthermore, these relationships have been fit to second order polynomials shown by the black and gray lines, which shows that there are clearly size and latitude differences between these composites. These results suggest that the differences in the WPRs between intensifying and weakening systems is likely due to differences in size and latitude between intensifying storms on average are smaller. Several studies have shown that the circulation associated with TCs become larger the longer the storm exists (Knaff et al. 2006; Cocks and Gray 2002; Weatherford and Gray 1988; Merrill 1984). The results suggest that the majority of storms intensifying early in their life-cycle when on average they are smaller and at lower latitude and weaken latter in their life-cycle when they are larger and at higher latitude. The results however suggest that it is the size differences that are most important. In the intensity range of 64 to 100 kt the sizes are ~.30 standard deviations smaller for the intensifying composite, but only a couple of degrees latitude equatorward. This result will be examined further in the next section discussing the development of unified WPRs.

5. Unified wind-pressure relationships

A unified WPR to predict MSLP is derived using multiple linear regressions where the predictors tested are TC size, latitude and intensification trend. The intensity trend predictor, while added as a potential predictor in the multiple regression approach,

resulted in less than .01% reduction of the variance when latitude and size were included as predictors. For this reason, intensity trend is not considered. This further emphasizes that intensity trend is not independent of the factors size, and latitude. The resulting multiple regression equation is

$$(7) \qquad MSLP = 23.286 - 0.483V_{srm} - \left(\frac{V_{srm}}{24.254}\right)^2 - 12.587 * S - 0.483 * \phi + P_{env} \ ,$$

where V_{srm} is the maximum wind speed adjusted for storm speed, S (i.e., = V_{500}/V_{500c})is the normalized size parameter discussed in Section 3, and ϕ is latitude (degrees). When applied to the individual cases used to make the composites, this equation explains 94% of the variance with a Root Mean Square Error (RMSE) of 5.8 hPa and a mean absolute error (MAE) of 4.4 hPa. For comparison, the standard Dvorak curve for the Atlantic explained 91% of the variance with a RMSE of 7.1 hPa and a MAE of 5.4 hPa.

One could solve Eq. 7 for V_{srm}, but analogous to solving for the gradient wind, the solution has two roots. The WPR can also be derived as a separate regression equation to estimate V_{max} given ΔP. In the development of this regression equation (Eq. 8), the square root of ΔP is used as a predictor in addition to ΔP, size and latitude.

$$(8) \qquad V_{\max} = 18.633 - 14.960S - 0.755\phi - 0.518\Delta P + 9.738\sqrt{|\Delta P|} + 1.5c^{0.63},$$

where c is the storm translation speed. Applying this relationship to the individual fixes explains 93% of the variance of the wind speed and results in a MAE of 6.0 kt and a RMSE of 7.8 kt. Again for comparison, the Atlantic Dvorak curve explains 90 % of the variance, with MAE of 7.6 kt and RMSE 9.8 kt. Because S is a function of V_{max}, a good

estimate of V_{max} is needed otherwise Eq. 8 should be iterated to a solution of V_{max}. Convergence within a 1 kt is usually obtained in 2 iterations.

The WPRs developed in this section (i.e., Eq. 7 and Eq. 8) account for the influence of TC size and latitude, storm motion and environmental pressure when estimating MSLP and $V_{max.}$ Figure 12 shows the dependent relationships from Eq. 7 and Eq. 8. Both relationships can be used in operations to help with the assignment of V_{max}, given a measurement of MSLP, and to estimate MSLP when V_{max} has been estimated (e.g., Dvorak intensity estimates). Since there is still considerable uncertainty with the various observations (satellite estimates, reconnaissance wind reduction, wind averaging periods, etc.), these equations can also be used to add consistency to operational V_{max} and MSLP estimates. Furthermore, since both Eq. 7 and Eq. 8 account for P_{env}, TC size, and latitude - the same factors that account for the differences between TC basins, thus these equations can be applied to any TC basin. Under that premise, these relationships are used in the next section to examine other WPRs used at operational centers.

A possibly more important used of these equations is to offer an improved way to estimate intensities for climatological reanalysis of TC intensities. There is an increasing need to reanalyze the best track intensities in all basins since these historical records are being used to assess climate change (e.g., Webster et al, 2005; Emanual 2005). While the Atlantic basin best track including intensity has been reanalyzed from 1850-1910 (Landsea et al. 2004), future reanalysis of intensities will be aided by the results presented here. With this type of application in mind, Section 7 presents a comparison of results generated by Eq. 8 with the method used in Landsea et al. (2004).

6. Reexamination of operational wind-pressure relationships

The first operational WPR examined is Dvorak (1975, 1984) for the Atlantic, which is used for estimating MSLP in the Atlantic, Eastern Pacific and Central Pacific. To examine the Dvorak (1975) Atlantic WPR, the published tables were fit to a function $MSLP = 1021.36 - 0.36V_{\max} - \left(\frac{V_{\max}}{20.16}\right)^2$, which introduces a MAE of 0.7 hPa, RMSE of 0.8 hPa, and bias of 0.1 hPa to the Dvorak WPR table. The developmental data were then passed through this function. The results are then compared with MSLP computed from Eq. 7 using the observed environmental pressure as well as the sample average environmental pressure for P_{env}. Those results were then compared with the observed MSLP and MAE, RMSE and bias, shown in Table 2. Results that are statistically different, assuming 211 degrees of freedom (*df*) (i.e., $df = -n\log(r_1)$, where r_1 is the lag 1 auto correlation) and a standard two-tailed student's t-test, than those produced by equation 7 are italicized (95 % level) and boldfaced (99% level) in the table.

Using Eq. 7 along with the observed environmental pressure showed improvement over the Atlantic Dvorak WPR relationship. Even the use of mean environmental pressure in Eq 7 instead of the observed environmental pressure yielded slightly better results. The effectiveness of the Dvorak WPR is however remarkable considering that it was developed using mostly western Pacific data, but adjusted upward for the average differences in environmental pressure (Harper 2002). There are however a couple of caveats associated with these results. The first is that the Dvorak WPR is used operationally in these basins and there may be a built in dependence (i.e., using this relationship to assign V_{max} some of the time) as suggested by Harper (2002). The second

is that Eq. 7 is not completely independent. Independent results are presented later in this paper.

The next operational WPR examined is that of Koba (1990). Using a similar approach the tabular values of ΔP (assuming P_{env} = 1010 hPa) were fit to a function, $\Delta P = 6.22 - 0.58V_{\max} - \left(\frac{V_{\max}}{31.62}\right)^2$, where V_{max} is the 1-minute sustained wind associate with the Dvorak current intensity (CI) number. Thus, this study does not consider the conversion of 1-minute to 10-minute averaging times used in Koba et al. (1990) or by the Japanese Meteorological Agency. This function introduces a MAE of 0.8 hPa, RMSE of 0.9 hPa and bias of 0.4 hPa to the Koba et al. WPR Table. These are then compared to Eq. 7 in a similar manner as before. The results and statistical significance of this comparison are shown in Table 2. The Koba et al. (1990) relationship is not a good relationship for these data because it has a large and systematic bias. A closer inspection of the biases shows that they are very similar to the changes in ΔP seen between composites of average and small TC's compared with large TCs. This result along with the observation that TCs in the western Pacific are generally larger than those in the Atlantic (Merrill 1984) suggest that the Koba et al. (1990) sample is generally of larger storms. If just the storms in the large composite are considered, the Koba et al. (1990) WPR seems good (i.e., not statistically significant at the 90% percent level); RMSE is 7.0 hPa and MAE is 5.7 hPa with a bias of -2.2. For comparison, Eq. 7 produced RMSE of 8.1 and MAE of 6.6 and had a bias of -5.3 for the large storm sample. Indirectly, this further implies that the Koba et al. dataset likely consisted of generally larger storms.

The next WPR examined is the A&H, which should have similar properties to the Koba et al. (1990) WPR (i.e., similar to the large composite sample). Again 1010 hPa is

used for the environmental pressure and the published function is $\Delta P = -\left(\frac{V_{\max}}{6.7}\right)^{1.553}$.

The error statistics associated with the application of this WPR to this study's data and its rather poor performance are shown in Table 2. Since the Koba et al. (1990) results suggest that the West Pacific sample may contain larger storms, error statistics are also calculated for the large composite data; RMSE is 12.5 hPa MAE is 9.67hPa with a bias of -7.4 hPa – all of which are statistically significant at the 99% level. These values are very similar to the comparison with the whole dataset, suggesting the A&H WPR may not be as valid as either Eq. 7 or the Koba et al. (1990) WPR. Interestingly there is a negative bias throughout the entire intensity range with the largest errors occurring for very intense storms. The estimates of ΔP made by the A&H WPR tend to be 20 hPa too low for V_{max} above 120 kts. It therefore appears that the A&H WPR is a bad fit. This last point is expanded upon in Appendix A where the raw A&H data is reexamined.

In Australia there is different WPR used at each TC forecast office. Perth uses the A&H WPR, Darwin uses Love and Murphy (1985) WPR, where $\Delta P = 6.37 - 0.54V_{\max} - \left(\frac{V_{\max}}{43.03}\right)^2$, and Brisbane uses a WPR table attributed to Crane $\Delta P = 5.82 - 0.50V_{\max} - \left(\frac{V_{\max}}{22.20}\right)^2$. The errors introduced by creating functional forms are MAE of 0.4 hPa, RMSE of .52 hPa, and a bias of 0.4 hPa for the Love and Murphy WPR and MAE 0.7 hPa, RMSE of 1.0 hPa and a bias 0.7 hPa for the Crane WPR. Using the same methodologies as above, both of these WPRs are compared to results from Eq. 7 as shown in Table 2.

The Love & Murphy WPR produces good error statistics, but the overall biases are a result of large negative biases associated with weaker storms and large positive biases, particularly above intensities of 90 kt (i.e., Dvorak T-no = 5.0). Since cyclones forecast by Darwin tend to be at low latitude and small, this WPR is similar to that of Lander and Guard (1996) created specifically for midget TCs. To examine the regional latitude effect, this WPR is then compared with the low latitude composite cases. , Doing so resulted in similar statistics that are statistically significant at 95% level; RMSE 8.9hPa, and MAE 7.4 hPa, bias -4.0hPa, compared to RMSE of 7.4, MAE of 5.9 and a bias of -4.5 from Eq. 7. Similarly, a comparison was made with the small composite data resulting in RMSE of 8.7 hPa, MAE of 7.2 hPa, and a bias of -5.4 hPa compared to RMSE of 7.0 hPa, MAE of 5.1 hPa and a bias of -3.3 hPa. These differences too were significant at the 95% level.

The WPR used at Brisbane has similar characteristics as the A&H WPR (Harper 2002) and as shown in Fig 1. Error statistics for this WPR are shown in Table 2. Inferring a similarity with the Western Pacific, this scheme was also examined using the large composite resulting in a bias of -5.1 hPa, RMSE of 9.45 hPa and MAE of 7.5 hPa. Thus, this methodology has similar performance characteristics as the A&H WPR.

In summary there are five WPRs used in operations throughout the world. Each was examined for their ability to perform better than the relationship given in Eq. 7. One of the five methods, the Atlantic Dvorak performed well when compared to results produced by Eq. 7. The Dvorak Atlantic relationship from Dvorak (1975, 1984) produced good results for the entire developmental dataset. Two other relationships performed well for subsets of the developmental data. The Koba et al. (1990)

relationship is valid for a large sized subset of storms and the Love and Murphy (1985) WPR relationship seems valid for the combination of small and low latitude storms, though Eq. 7 provides a better fit to the developmental data. The WPR attributed to Crane used at the Brisbane Tropical Cyclone Centre performed poorly versus the developmental sample and other size-based sub samples, and thus a change in operational WPRs should be considered.

Finally, the A&H WPR has a large negative bias in V_{max} for intense storms that does not seem to be supported by our dataset nor by the developmental dataset used in Koba et al. (1990). This result suggest that the replacement of the Dvorak (1975) West Pacific WPR table by that of A&H in Dvorak (1984) may have been unjustified. Given the rather limited justification for the use of A&H in the West Pacific (i.e., Shewchuk and Weir 1980; Lubeck and Shewchuk 1980), and the results from the Koba et al. (1990) WPR presented here, the use of the A&H WPR appears unsupported by the data. The problem with this method can be attributed to the methodology used to fit the data as discussed in Appendix A. In regions where the A&H WPR is used, its use should reconsidered and possibly replaced by that of Eq. 7, the Koba et al. (1990) WPR, or at very least the West Pacific WPR table published in Dvorak (1975).

Furthermore, regarding recent climatological studies, evidence suggests that use the A&H WPR to assign wind speeds given the aircraft estimate of MSLP has resulted in a systematic wind speed bias (too low) in the West Pacific TC climatology during the time of its use at JTWC (~1974-1987). Figure 13 shows the MSLP estimated from aircraft vs. the best track wind speeds in the western North Pacific for 1966-1973 and 1974-1987 along with the best fit to the data and the A&H WPR. In operations it was

routine that surface winds were assigned using observed MSLP in WPRs. This figure shows that in the later period (1974-1987) that the A&H WPR is used to assign maximum surface wind speeds. This results in the western North Pacific best track intensity estimates being too low in the years 1974-1987, particularly for the more intense storms. These findings offer an alternative explanation for some of the upward trends in TC intensity reported in North West Pacific (Emanuel 2005; Webster et al. 2005). Ironically, this implies that the West Pacific best track V_{max} estimates for the stronger storms may have become more accurate without aircraft reconnaissance, somewhat contradictory to the results of Martin and Gray (1993).

7. Wind-pressure relationships used for climatological reanalysis

While operational users usually assign a pressure given a wind, the opposite is done when meteorologists reanalyze TC intensities. Often there is an observed or estimated MSLP from reconnaissance or surface/ship observations, but no or limited measures of the TC wind speed. The tabular forms of the operational tables are sometimes used to do this type of reanalysis, but as shown above, these operational tables sometimes result in considerable bias and error. Equation 8 offers an alternative to the operational tables and can be iterated to a stable solution for V_{max} given MSLP.

Recently the Atlantic best tracks were reanalyzed and extend backward in history for the period 1851-1910. There were four WPRs used for this reanalysis (Landsea et al 2004), which were developed from the aircraft era of the best track dataset (1970-1997)

in regions known to have routine reconnaissance. These WPR (shown in Figure 1b) will now be examined in a similar way as the WPRs used in operations, but with respect to V_{max} (i.e., Eq. 8) for comparisons. These comparisons again make use of the observed environmental pressure and the sample mean or climatological pressure.

Results of this analysis are shown in Table 3. In the region south of 25 N both the Landsea et al relationship and Eq. 8 performed well with slightly negative biases and MAEs below 7.5 hPa. It is interesting to note that the use of the observed environmental pressure south of 25N resulted in significant improvements to both schemes. In the Gulf of Mexico, Eq. 8 outperforms the Landsea et al. equations, and again the use of environmental pressure results in smaller errors in Eq.8 as well as the Landsea et al. equation. Results from Eq. 8 are shown to produce superior results in the Atlantic regions between 25 N and 35N. In this region, the use of the observed environmental pressure has a negative effect on the Landsea et al. relationships. In the region poleward of 35N region, Eq 8 is again superior to the Landsea et al. approach. Also notice that there is more scatter in the data (i.e. larger RMSE) suggesting more size and environmental pressure variability in this poleward of 35N group. As a result, errors associated with both Eq. 8 and the Landsea et al. relationships increase dramatically in this higher-latitude region. For comparison the Atlantic Dvorak tables produced RMSE of 9.8 kt, MAE of 7.6 kt and a bias of 0.8 kt for the entire developmental dataset.

In summary, the Landsea et al. equations do an admirable job of estimating the winds from the pressure equatorward of 25 N, while the Landsea et al. WPRs for Atlantic storms north of 25 N and for the Gulf of Mexico have larger errors and lower correlation than those produced by Eq. 8. In all cases, the results from Eq. 8 improve on the

Landsea et al. equations. This suggests that environmental pressure and cyclone size play a factor in the WPR, particularly north of 25N, and should be considered when reanalyzing TC intensity since 1948 when TC size estimates are available from the NCEP reanalysis data.

8. Independent results from 2005

To better ascertain the accuracy of Eq. 7 and Eq. 8 an independent dataset from the entire 2005 Hurricane Season is used to evaluate these equations. Similar results were also calculated using the Atlantic tables in Dvorak (1975, 1984). Results, shown in Table 4, suggest that the equations developed here perform significantly better than the operational Dvorak WPR. Pressures (winds) are more accurate by approximately 2 hPa (3 kt) for this 524 case sample.

Figure 14 shows predicted V_{max} given the MSLP using Equation 8 and the Dvorak WPR vs. the final best track V_{max} estimate (top) and the predicted MSLP using Equation 7 and the Dvorak WPR vs. aircraft measurement of MSLP (bottom). The scatter associated with the estimates made with Eq. 7 and Eq. 8 are smaller and the estimates have a better one to one correspondence with the observations than those making use of the Dvorak WPR. It is also noteworthy that the largest outliers (30 kt and 27 hPa) were associated with Hurricane Wilma, which at that time had a 2 nm radius of maximum winds and 892 hPa MSLP. Large over estimation of V_{max} and under estimation of MSLP occurred with Hurricane Rita as its radius of maximum winds appeared to shrink as it approached land; in fact its MSLP was a record low for a storm hitting the coast with 100

kt winds. The errors associated with these two independent cases suggest that information about the radius of maximum winds could likely improve these relationships even further.

9. Summary and Recommendations

This purpose of this work was to reexamine the issue of TC WPRs using more recently collected and higher quality datasets along with additional environmental factors that are measurable in an operational setting. While it is recognized that other factors (i.e., radius of maximum wind, secondary wind maxima, flight level to surface wind reduction, asymmetries, and other radial wind profile variations) will influence the MSLP relationship to the wind, these factors are not easily and accurately obtained in either an operational setting and/or only occasionally in a post analysis setting. Such factors therefore were not considered in this study. As a result, there is still considerable scatter in these new WPRs when these factors, particularly variations of the radius of maximum wind, are influencing the WPR.

Results indicate that by using information about TC location (i.e., latitude) along with estimates of size and of environmental pressure estimated from operational analysis or reanalysis fields, the MSLP can be estimated from the V_{max} within 5 to 6 hPa and the wind can be estimated from the MSLP within 7 to 8 kt. These relationships have been shown to be better than what is being used operationally and for reanalysis of past events. In addition, the data have shown that several operational WPRs have substantial

shortcomings and their operational use should be reconsidered. It was also found that the equations used to reanalyze Atlantic TCs (i.e., Landsea et al. (2004)) preformed rather well equatorward of 25 N. Estimates of winds in the open Atlantic poleward of 25N and in the Gulf of Mexico result in significantly larger errors than the methodology presented here (i.e., Eq. 8).

Wind-pressure relationships have left their mark on the global TC climatology in those basins that had routine aircraft reconnaissance and thus good estimates of MSLP. Fortunately, the actual WPRs used and the methodologies to assign V_{max} have evolved and improved, but this has resulted in considerable errors and inconsistencies in the best track intensities of the past. This is an important point because the best track intensities are now being examined for climatic trends (e.g., Webster et al 2005; Emanuel 2005). While the WPRs presented in this paper still result in considerable scatter, their application to past data will nonetheless result in an objective and homogeneous measure of TC intensity. Only by removing the inhomogeneous nature of best track intensities, whether by this method or some other method, can climatic trends in numbers and intensities be properly quantified.

The results of this study also inspire the following recommendations. 1) The unified equations for the WPR should be considered for operational use in all basins. This would help better assign MSLP that is provided to initialize forecast models as well as result in uniform intensity estimates. 2) The A&H WPR and the Crane WPR, which is similar, be replaced in all basins currently using this relationship. Further justification is given in Appendix A. 3) The west Pacific best tracks should be reanalyzed during the period when reliable measurements of MSLP were available. Doing so would likely

increase the number of strong typhoons (1974-1987) and thus reduce the upward intensity trends observed in the best track (1970-2004) as discussed in Webster et al. (2005) and Emanuel (2005). 4) The unifying equations (Eq. 7, 8) should be utilized to reanalyze the best tracks in the Atlantic when the NCEP reanalysis and MSLP estimates are available (1948-present). This would help to provide a more consistent and accurate estimate of maximum surface winds in the best track dataset.

Acknowledgements: This research was supported by *NOAA grant NA17RJ1228.* The views, opinions, and findings contained in this report are those of the author(s) and should not be construed as an official National Oceanic and Atmospheric Administration or U.S. Government position, policy, or decision. The authors thank the three anonymous reviewers for their suggestions and comments, which have improved the paper. The authors also would like to thank Bruce Harper for providing the digital Atkinson and Holliday (1975) dataset used in Appendix A.

Appendix A: The Atkinson and Holliday wind-pressure relationship revisited:

The A&H WPR is reexamined using the original tabular data listed in Atkinson and Holliday (1975). The first step is reproducing the prior result. Using the raw data, the function $V_{\max} = C(1010 - MSLP)^x$ was fit to see if the original relationship could be reproduced. The results of this fit, $V_{\max} = 6.6(1010 - MSLP)^{.65}$, were slightly different than the publish version (i.e., $V_{\max} = 6.7(1010 - MSLP)^{.644}$, but close enough to confirm that A&H WPR was fit to the raw data without first binning by intensity.

To examine the effect of binning the data, the raw data are sorted by $V_{\max}$, binned every 6 points and refit to the same function. The result, $V_{\max} = 4.4(1010 - MSLP)^{.76}$, is much different than the original published fit. Finally the functional form used previously in this paper is fit (i.e., $\Delta P \approx aV_{srm}^2 + bV_{srm} + C$) so that direct comparison with the WPR of Koba et al. (1990) can be made. The results

$\Delta P = 11.48 - 0.73V_{\max} - \left(\frac{V_{\max}}{107.21}\right)^2$ are nearly identical, while slightly more linear, to the fit to the WPR table published in Koba et al (1990) (i.e., $\Delta P = 6.22 - 0.58V_{\max} - \left(\frac{V_{\max}}{31.62}\right)^2$). It also is found that the all of formulations that make use of the binned data and the Koba et al. WPR produce a better fit to the raw data than the A&H WPR equation. Table A1 shows the relevant error statistics associated with each fit.

The bias introduced by the A&H WPR is clearly shown in Figure A1, which shows the published A&H WPR, the fit to the binned Atkinson and Holliday (1975) data

assuming cyclostrophic form, and the Dvorak (1975) for intensities from 25 to 170 kts. Note the other WPRs developed using the binned data discussed above as well as the Koba et al. WPR are nearly identical (within 1 hPa) to cyclostrophic fit shown in Fig. A1. This last point is remarkable because the V_{max} data in A&H were likely overestimated, particularly at elevated sites (Harper 2002). Figure A1 alone suggests that the prolonged use of the A&H WPR in the West Pacific (1974-1987) has resulted in a negative bias in the best track intensities.

Appendix B: Dvorak CI curves for various composites:

From a combination of the Equations 7 and 8 and the composite averages Dvorak WPR tables are formulated in terms of Current Intensity Number (CI) vs ΔP. Three tables are listed for the three latitude belts used in this study. Table B1, Table B2, and Table B3 are valid for storms located equatorward of 20^{o}, from 20^{o} to 30^{o} latitude and for greater than 30^{o} latitude, respectively.

References:

Atkinson, G. D., and C. R. Holliday, 1977: Tropical cyclone minimum sea level pressure/maximum sustained wind relationship for the western North Pacific. *Mon. Wea. Rev*., **105**, 421-427.

Atkinson, G. D., and C. R. Holliday, 1975: Tropical cyclone minimum sea level pressure – maximum sustained wind relationship for western North Pacific. FLEWEACEN Tech. Note: JTWC 75-1, US Fleet Weather Central, Guam, 20 pp. [Available from National Meteorological Library, GPO Box 1289, Melbourne, Vic, 3001, Australia.]

Cocks S. B. and W. M. Gray, 2002: Variability of the outer wind profiles of western North Pacific typhoons: classifications and techniques for analysis and forecasting. *Mon. Wea. Rev.,* **130**, 1989–2005.

Dvorak, V. F., 1975: Tropical cyclone intensity analysis and forecasting from satellite imagery. *Mon. Wea. Rev*., **103**, 420-430.

____, 1984: Tropical cyclone intensity analysis using satellite data. NOAA Technical Report NESDIS 11, 45pp.

Emanuel , K., 2005: Increasing destructiveness of tropical cyclones over the past 30 years. *Nature*, **436**, 686-688.

Franklin, J. L. , M.L. Black, and K. Valde, 2003: GPS dropwindsonde wind profiles in hurricanes and their operational implications. *Wea. Forecasting*, **18**, 32-44.

Gross, J. M., M. DeMaria, J. A. Knaff and C. R. Sampson, 2004: A new method for determining tropical cyclone wind forecast probabilities, Preprints, *26th Conference on Hurricanes and Tropical Meteorology*, Miami, FL,425-426.

Harper, B. A., 2002: Tropical cyclone parameter estimation and the Australian region – wind-pressure relationships and related issues for engineering planning and design – A discussion paper. Systems Engineering Australia Pty Ltd (SEA) for Woodside Energy Ltd, SEA Rep. No. J0106-PR003E, Nov, 83pp. [Available from Systems Engineering Australia Pty Ltd, 7 Mercury Ct, Bridgeman Downs, QlD 4035, Australia.]

Hess, S. L, 1959: *Introduction to theoretical meteorology*. Holt, Rinehart and Winston, New York, 362pp.

Jarvinen, B. R., C. J. Neumann, and M. A. S. Davis, 1984: A tropical cyclone data tape for the North Atlantic Basin, 1886-1983: Contents, limitations, and uses. NOAA Tech. Memo., NWS NHC – 22, 21 pp. [Available from NTIS, Technology Administration, U.S. Dept. of Commerce, Springfield, VA 22161.]

JTWC, cited 2006: Tropical Cyclone Best Track Data Site. [Available online from http://www.npmoc.navy.mil/jtwc/best_tracks/btwplink.html]

Kalnay E. , M. Kanamitsu, R. Kistler, W. Collins, D. Deaven, L. Gandin, M. Iredell, S. Saha, G. White, J. Woollen, Y. Zhu, A. Leetmaa, B. Reynolds, M. Chelliah, W. Ebisuzaki, W. Higgins, J. Janowiak, K.C. Mo, C. Ropelewski, J. Wang, R. Jenne and D. Joseph. 1996: The NCEP/NCAR 40-Year Reanalysis Project. *Bull. Amer. Meteor. Soc.*, **77**, 437–471.

Kepert J., 2001: The dynamics of boundary layer jets within the tropical cyclone core. Part I: Linear theory. *J. Atmos. Sci.*, **58,** 2469–2484.

Kepert, J. and Y. Wang., 2001: The dynamics of boundary layer jets within the tropical cyclone core. Part II: Nonlinear enhancement. *J. Atmos. Sci.*, **58,** 2485–2501.

Knaff, J. A. , M. DeMaria, and J. P. Kossin, 2003: Annular hurricanes. *Wea. Forecasting*, **18**, 204-223.

Kossin J.P., 2002: Daily hurricane variability inferred from GOES infrared imagery. *Mon. Wea. Rev.*, **130**, 2260–2270.

Koba, H., T. Hagiwara, S. Asano, and S. Akashi, 1990: Relationships between CI number from Dvorak's technique and minimum sea level pressure or maximum wind speed of tropical cyclone. *J. of Met. Research*, **42**, 59-67. (in Japanese)

Guard, C. P., and Lander, M. A., 1996: A wind-pressure relationship for midget TCs in the western North Pacific. *1996 Annual Tropical Cyclone Report*, Naval Pacific Meteorology and Oceanography Center/ Joint Typhoon Warning Center, p. 311. [available online at http://www.npmoc.navy.mil/jtwc/atcr/atcr_archive.html.]

Landsea, C. W., C. Anderson, N. Charles, G. Clark, J. Dunion, J. Fernandez-Partagas, P. Hungerford, C. Neumann, and M. Zimmer, 2004: The Atlantic hurricane database re-analysis project: Documentation for 1951-1910 Alterations and additions to the HURDAT. *Hurricanes and Typhoons Past, Present and Future.* R. J. Murname and Kam-Biu Liu, Eds., Columbia University Press, 177-221.

Love, G., and K. Murphy, 1985: The operational analysis of tropical cyclone wind fields in the Australian northern region. Bureau of Meteorology, Northern Territory

Region, Research Papers 1984-1985, Nov, 44-51. [Available from National Meteorological Library, GPO Box 1289, Melbourne, Vic, 3001, Australia.]

Lubeck, O. M. and Shewchuck, J. D., 1980: Tropical cyclone minimum sea level pressure maximum sustained wind relationship. NOCC/JTWC 80-1, USNOCC, JTWC, Pearl Harbor, HI, 96860. [Available from National Meteorological Library, GPO Box 1289, Melbourne, Vic, 3001, Australia.]

Martin, J. D. and W. M. Gray. 1993: Tropical cyclone observation and forecasting with and without aircraft reconnaissance. *Wea. Forecasting*, **8**, 519–532.

Merrill R. T., 1984: A comparison of large and small tropical cyclones. *Mon. Wea. Rev.*, **112**, 1408–1418.

Mueller, K. J., M. DeMaria, J. A. Knaff, J. P. Kossin, T. H. Vonder Haar, 2006: Objective estimation of tropical cyclone wind structure from infrared satellite data., *Wea. Forecasting*, in press.

Sampson, C. R., and A. J. Schrader, 2000: The Automated Tropical Cyclone Forecasting System (Version 3.2). *Bull. Amer. Meteor. Soc*., **81**, 1131-1240.

Schwerdt, R. W., F. P. Ho, and R. R. Watkins, 1979: Meteorological criteria for standard project hurricane and probable maximum hurricane wind fields, Gulf and East Coasts of the United States. NOAA Tech. Rep. NWS 23, 317pp. [Available from National Hurricane/Tropical Prediction Center Library, 11691 S.W. 117th St,Miami, Florida 33165-2149]

Shewchuck, J. D. and R. C. Weir, 1980: An evaluation of the Dvorak technique for estimating TC intensities from satellite imagery. NOCC/JTWC 80-2, USNOCC

,JTWC, Pearl Harbor, HI, 96860. [Available from National Meteorological Library, GPO Box 1289, Melbourne, Vic, 3001, Australia.]

Weatherford C. L., and W. M. Gray, 1988: Typhoon structure as revealed by aircraft reconnaissance. Part II: Structural variability. *Mon. Wea. Rev.*, **116**, 1044-1056.

Webster, P. J, G. J. Holland, J.A. Curry, and H.-R. Chang, 2005: Changes in tropical cyclone number, duration, and intensity in a warming environment. *Science*, **309**,1844-1846.

Willoughby, H. E. 1990: Gradient Balance in Tropical Cyclones, *J. Atmos. Sci.*, **47**, 265-274.

___, and M. E. Rahn, 2004: Parametric representation of the primary hurricane vortex. Part I: Observations and evaluation of the Holland (1980) model. *Mon. Wea. Rev.*, **132**, 3033–3048.

Figure Captions

Figure 1. Comparison of WPRs used operational throughout the world (a) and the WPRs used by Landsea et al (2004) as discussed in the text. Note all winds speeds are given in terms of 1-minute sustained winds and that the Dvorak CI number is used to compare WPRs where 10-minute average winds are the standard (e.g. Fiji, Japan and Australia).

Figure 2. Geographical location of the tropical cyclone fixes used in this study. Each hurricane symbol represents a fix.

Figure 3. Comparison between the maximum sustained 1-minute winds in the best track vs. the maximum 10-second wind reported at flight level 1995-2004.

Figure 4. The mean storm relative tangential velocity calculated from the NCEP Analyses and the NCEP reanalysis fields versus the average radius of 34-kt winds reported in the NHC advisories. The average is the mean radius of the nonzero quadrants for each advisory. Note that TC size and P_{env} are estimated from the NCEP reanalysis fields during 1989-2000, and from the NCEP operational analysis fields during 2001-2004.

Figure 5. Scatter plots of MSLP vs V_{max} (a), and ΔP vs. V_{max} (b).

Figure 6. Scatter plots of ΔP vs V_{max} (a), and ΔPvs. V_{srm} (b).

Figure 7. Plots of ΔP vs. V_{srm} for the three latitudinal composites.

Figure 8. A plot of the relationship between the tropical cyclone size parameter (V500/V500c) and the average 34-kt wind radii from operational advisories (1989-2004).

Figure 9. Plots of ΔP vs. V_{srm} for the three size based composites.

Figure 10. Plots of ΔP vs. V_{srm} for the two intensity trend-based composites.

Figure 11. Composite average storm relative maximum surface winds (V_{srm}) versus composite average tropical cyclone size (top) and average tropical cyclone latitude (bottom) are shown. Composites are stratified by 12-h intensity trends. The averages of storms with steady or weakening (intensifying) intensity trends are shown by the black (grey) points. Second order polynomial trend lines are added with the same shading.

Figure 12. Show the dependent results of Eq. 7 for predicting MSLP given V_{max} (a) and Eq. 8 for estimating V_{max} given MSLP (b).

Figure 13: MSLP vs best track maximum surface winds (Vmax) interpolated to the time of the observations and associated best fit relationships to these data for 1966 -1973 (a) and 1974-1987 (b). Also shown are the A&H (A&H) and Dvorak (1975) WPRs.

Figure 14: Scatter diagram of the independently predicted values of V_{max} using equation 8 (black boxes) and the Dvorak WPR (crosses) vs. observed values of MSLP from the operational best track (top). A similar scatter diagram for Eq.7 (black boxes) and the Dvorak WPR (crosses) vs. observed MSLP (bottom). Best linear fits for Eq.8 and Eq. 7 are shown with a solid black line in each respective panel with the associated variance explained at the bottom right. Best linear fits for the Dvorak WPR are shown by the gray dashed lines with the associated variance explained in the upper left. Sample includes 524 cases.

Figure A1: Various wind-pressure relationships plotted along with the Atkinson and Holliday (1977; 1975) developmental data. Shown are the A&H (1977), a fit to the binned raw data assuming a cyclostrophic form, and the Dvorak (1975) WPR. To plot these curves in terms of DP 1010 hPa is assumed to be the environmental reference pressure.

Table Captions

Table 1. Mean Statistics of the individual composites.

Table 2. Statistics associated with the Eq. 7 using the observed environmental pressure (P_{env}), Eq. 16 using the climatological environmental pressure (P_{clim}) from the sample, the Atlantic Dvorak, Koba et al (1990), A&H, Love and Murphy (1985) and Crane WPRs. Bias and error statistics that are statistically different than those produced by Equation 7 are shown as italicized and gray and italicized and boldface for the 95%, and 99% levels, respectively.

Table 3. Statistics (R^2, bias, RMSE and MAE) associated with the Eq. 8 using the observed environmental pressure (P_{env}), Eq. 8 using the climatological environmental pressure (P_{clim}) from each regional sub sample along with the appropriate Landsea et al. (2004) regional WPRs utilizing a reference pressure equal to 1013 and of P_{env} . Bias and error statistics that are statistically different than those produced by Equation 8 are shown as italicized and gray and italicized and boldface for the 95%, and 99% levels, respectively.

Table 4. Independent comparison of results obtained from Eq. 7 and Eq. 8 vs. the operational Dvorak Tables. Data includes 491 fixes from 12 Atlantic tropical cyclones and 1 East Pacific tropical cyclone during the 2005 season. Bias and error statistics that

are statistically different are shown as italicized and gray and italicized and boldface for the 95%, and 99% levels, respectively.

Table A1. Biases and MAE associated with the various fits to the raw Atkinson and Holliday (1975) dataset. Listed here are the published A&H WPR (1), the cyclostrophic form fit to the binned A&H data (2), the gradient fit for the binned A&H data (3) and for comparison the gradient fit to the Koba et al. (1990) WPR (4).

Table B1. Dvorak CI vs ΔP tables for storms occurring equatorward of 20^o latitude.

Table B2. Dvorak CI vs ΔP tables for storms occurring equatorward of 20^o to 30^o latitude.

Table B3. Dvorak CI vs ΔP tables for storms occurring poleward of 30^o latitude.

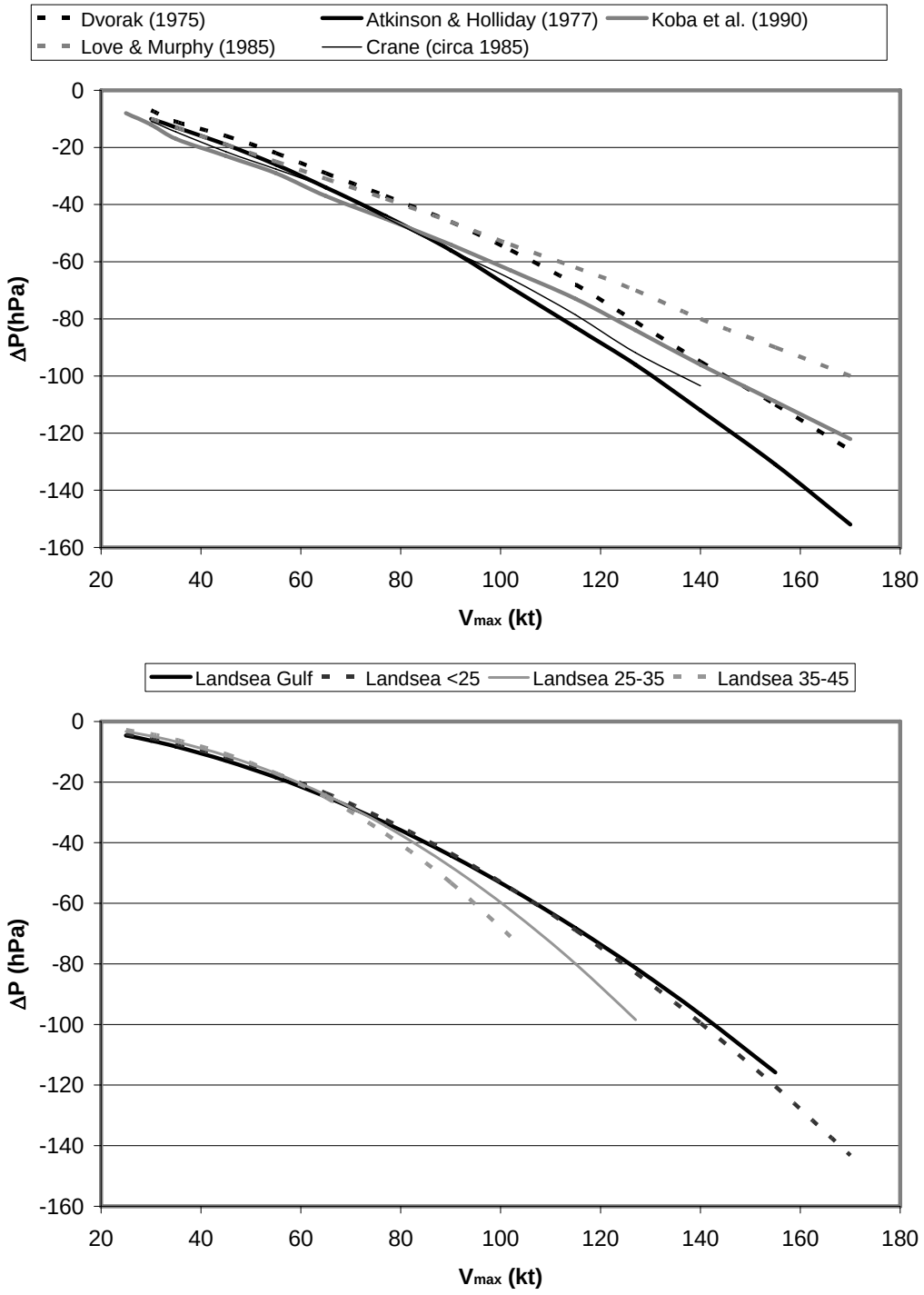

Figure 1. Comparison of WPRs used operational throughout the world (a) and the WPRs used by Landsea et al (2004) as discussed in the text. Note all winds speeds are given in terms of 1-minute sustained winds and that the Dvorak CI number is used to compare WPRs where 10-minute average winds are the standard (e.g. Fiji, Japan and Australia).

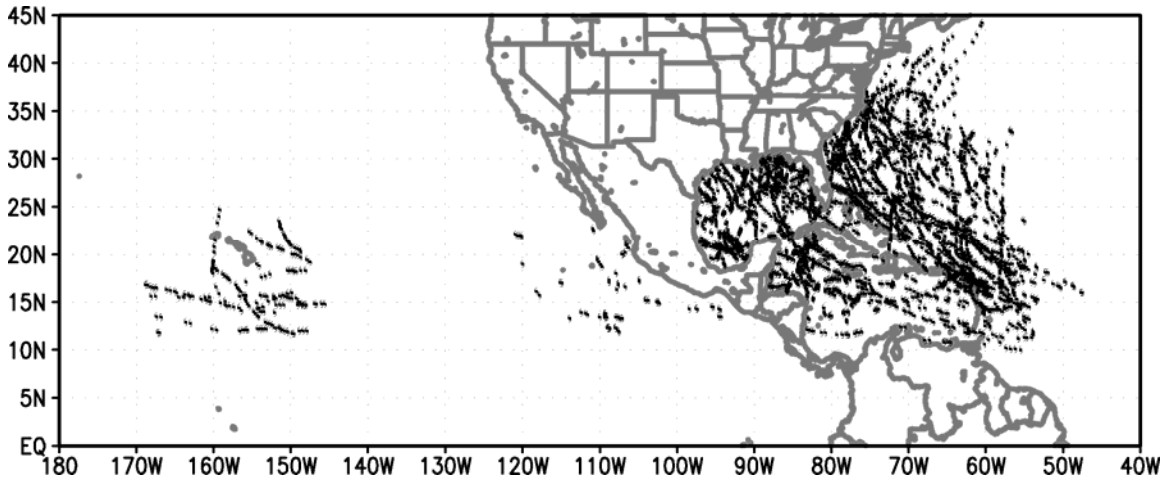

Figure 2. Geographical location of the tropical cyclone fixes used in this study. Each hurricane symbol represents a fix.

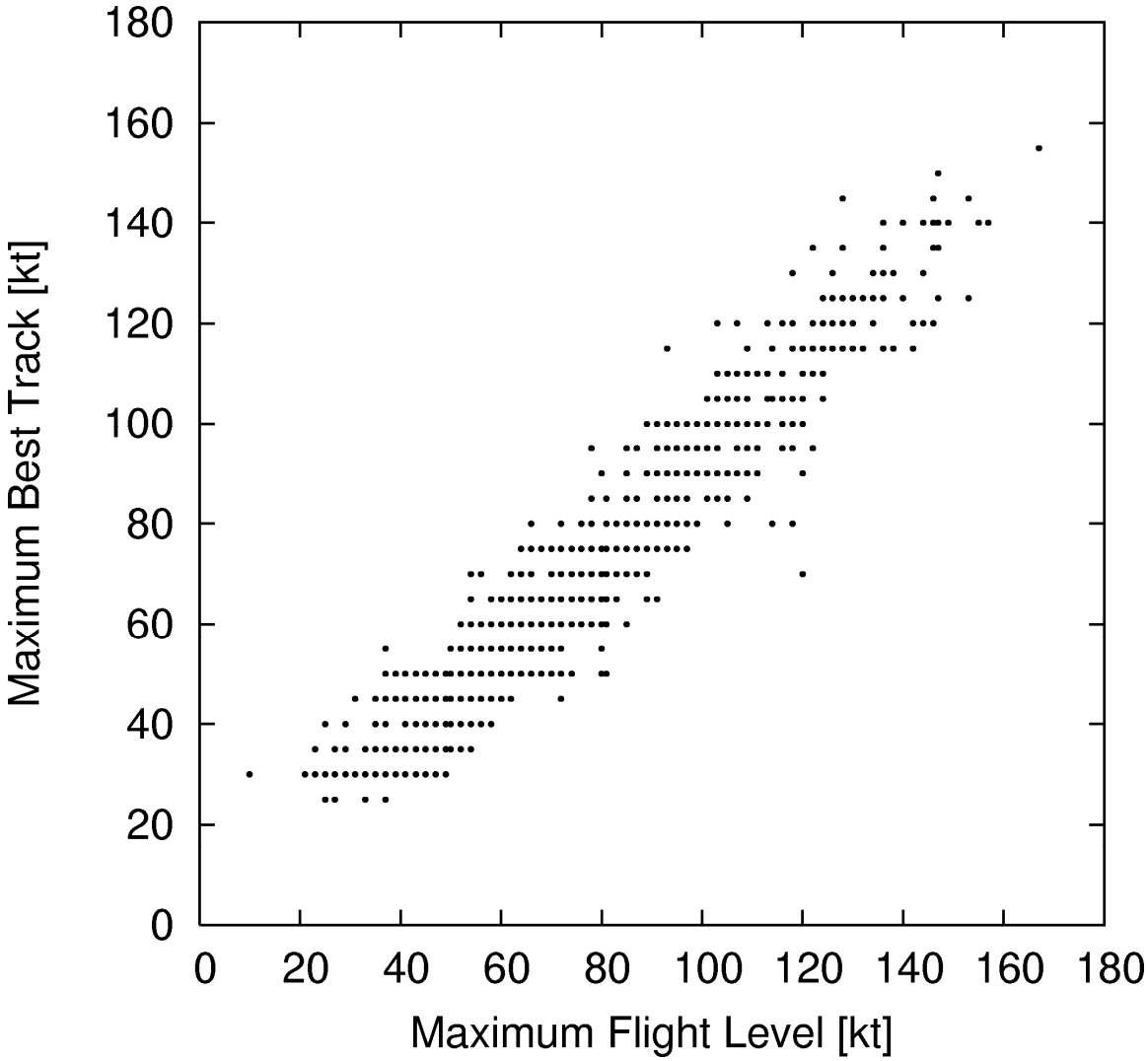

Figure 3. Comparison between the maximum sustained 1-minute winds in the best track vs. the maximum 10-second wind reported at flight level 1995-2004.

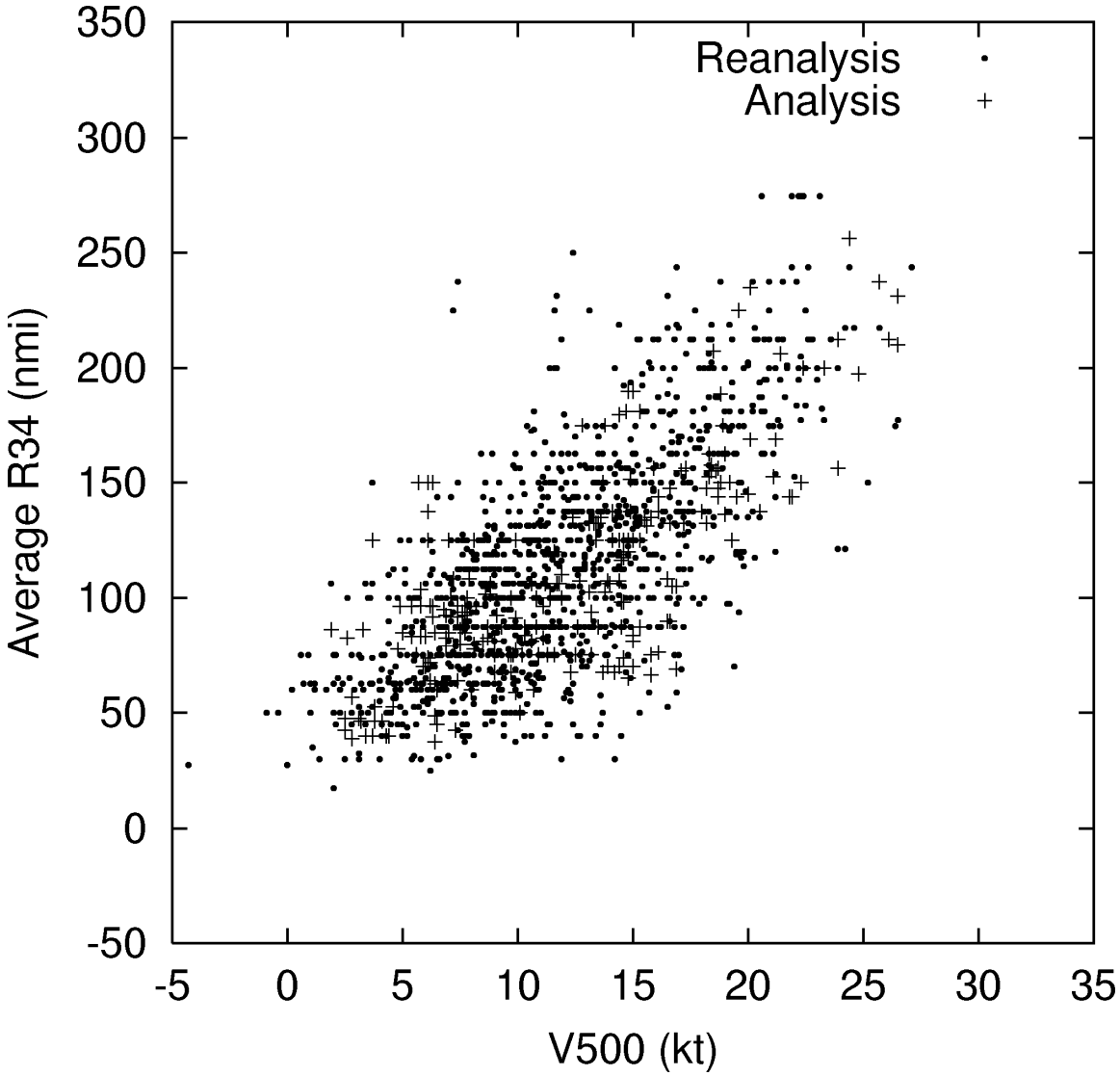

Figure 4. The mean storm relative tangential velocity calculated from the NCEP Analyses and the NCEP reanalysis fields versus the average radius of 34-kt winds reported in the NHC advisories. The average is the mean radius of the nonzero quadrants for each advisory. Note that TC size and P_{env} are estimated from the NCEP reanalysis fields during 1989-2000, and from the NCEP operational analysis fields during 2001-2004.

a.

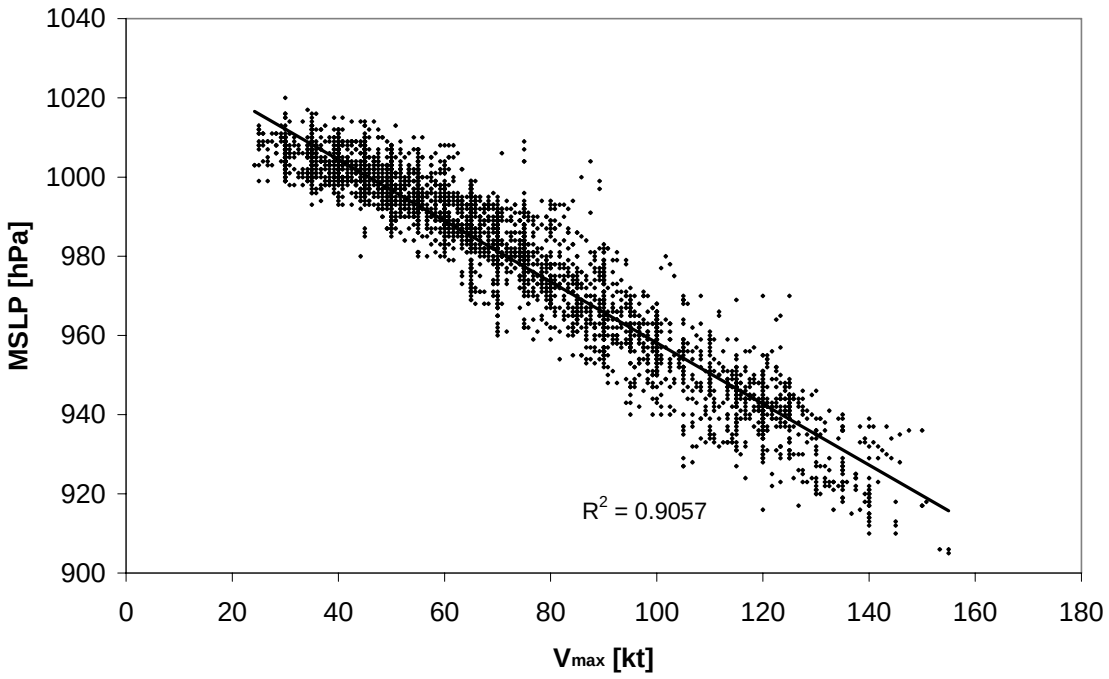

b.

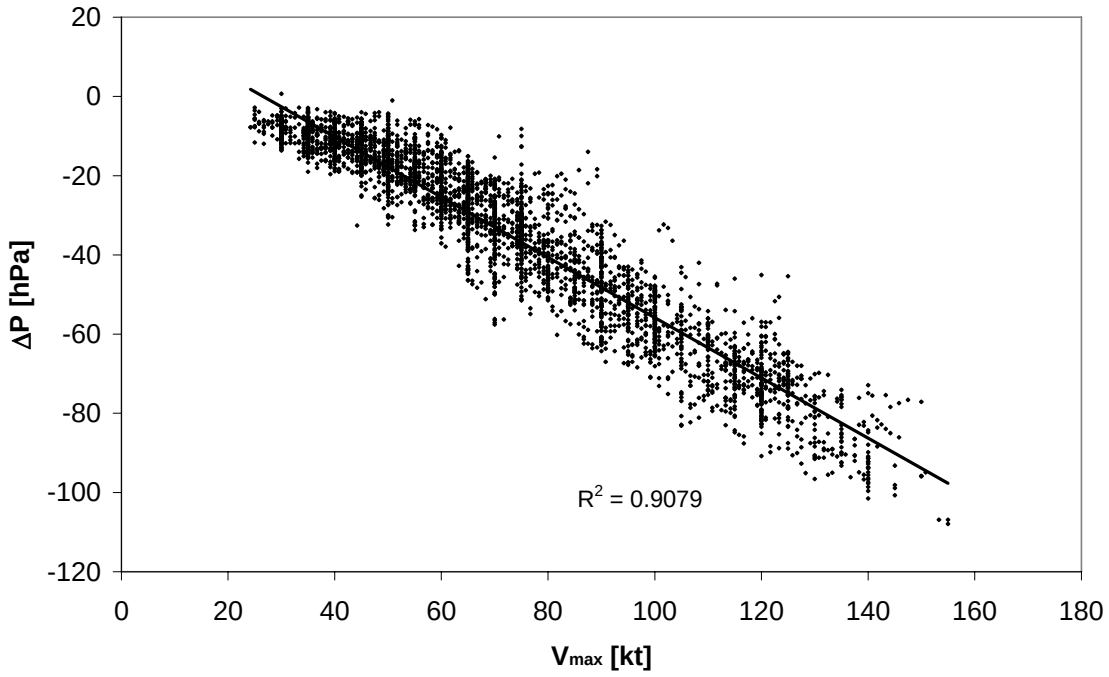

Figure 5. Scatter plots of MSLP vs V_{max} (a), and ΔP vs. V_{max} (b).

a.

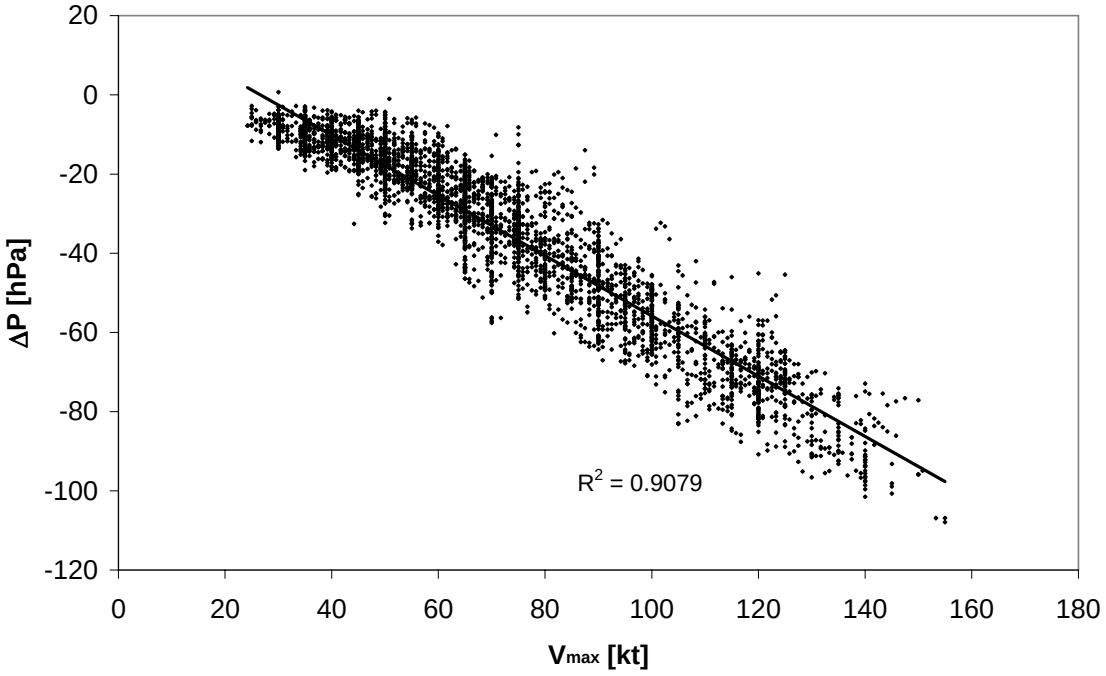

b.

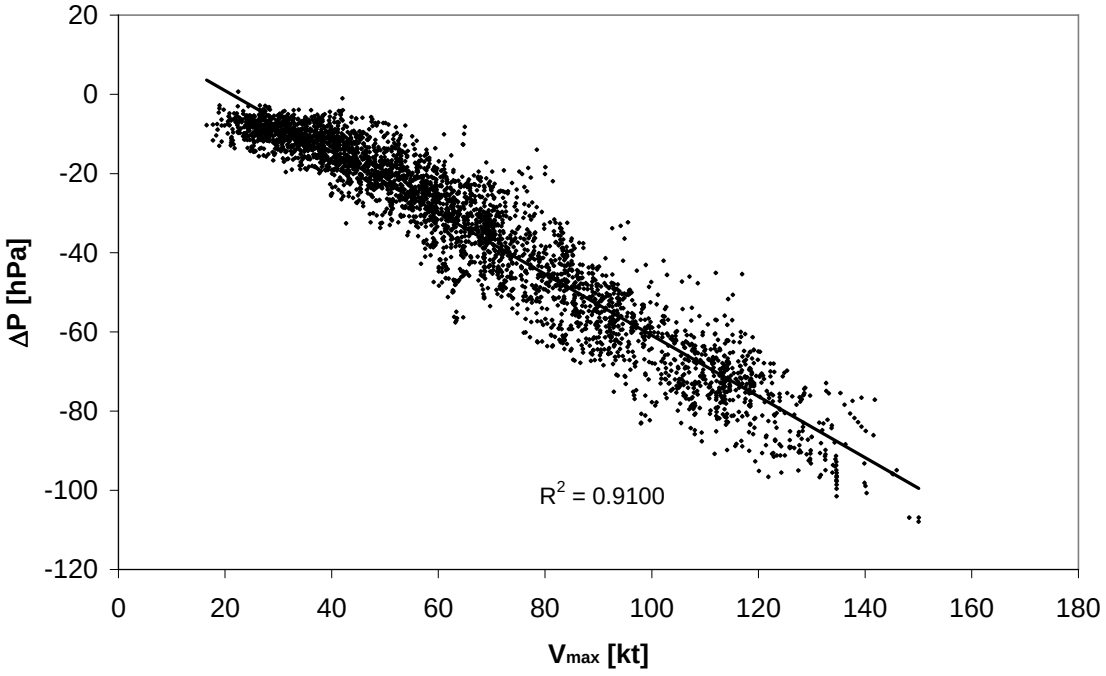

Figure 6. Scatter plots of ΔP vs V_{max} (a), and ΔPvs. V_{srm} (b).

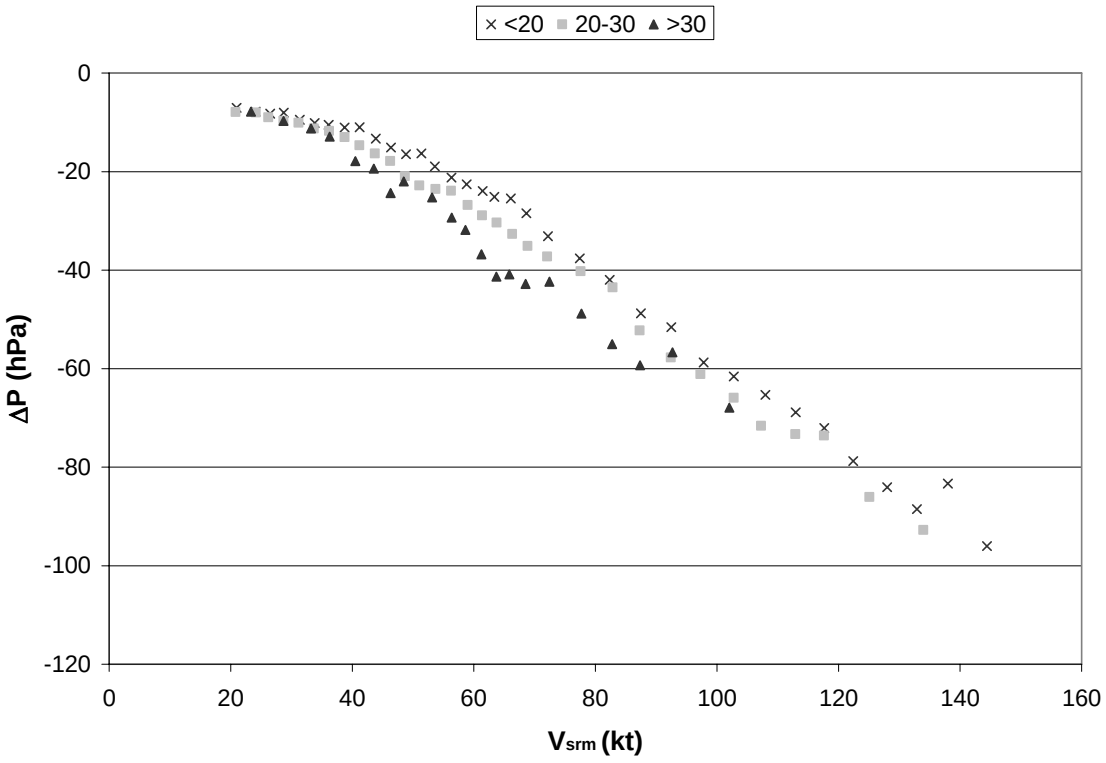

Figure 7. Plots of ΔP vs. V_{srm} for the three latitudinal composites.

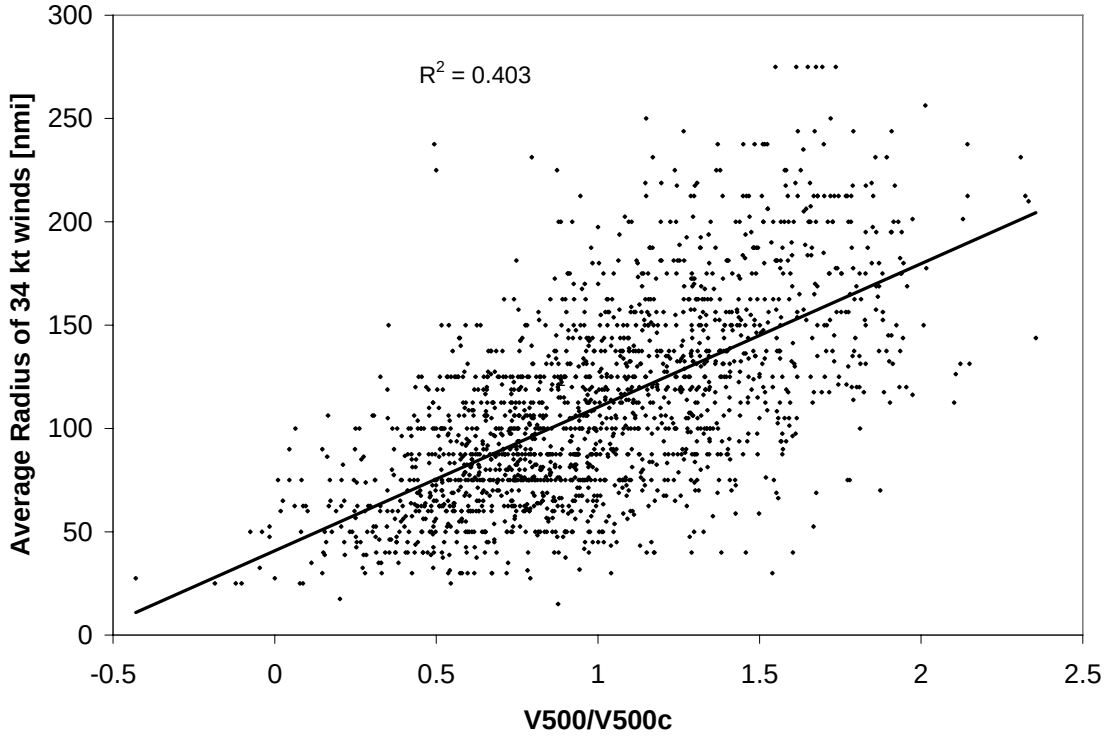

Figure 8. A plot of the relationship between the tropical cyclone size parameter (V500/V500c) and the average 34-kt wind radii from operational advisories (1989-2004).

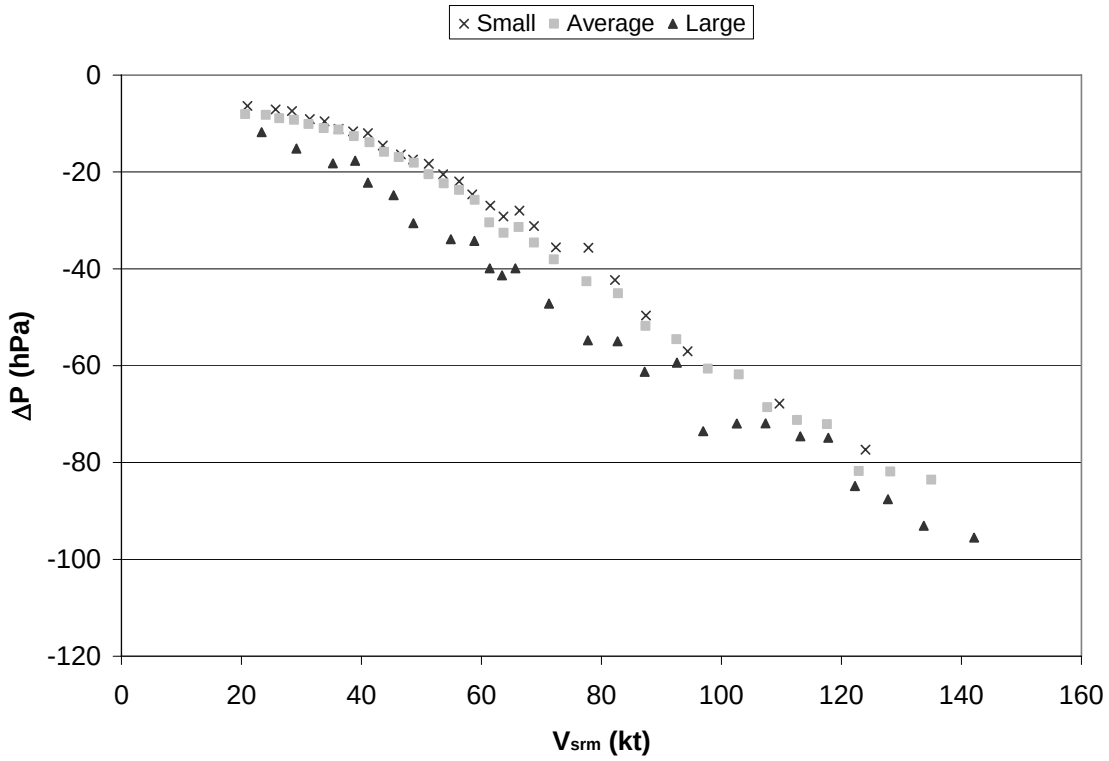

Figure 9. Plots of ΔP vs. V_{srm} for the three size based composites.

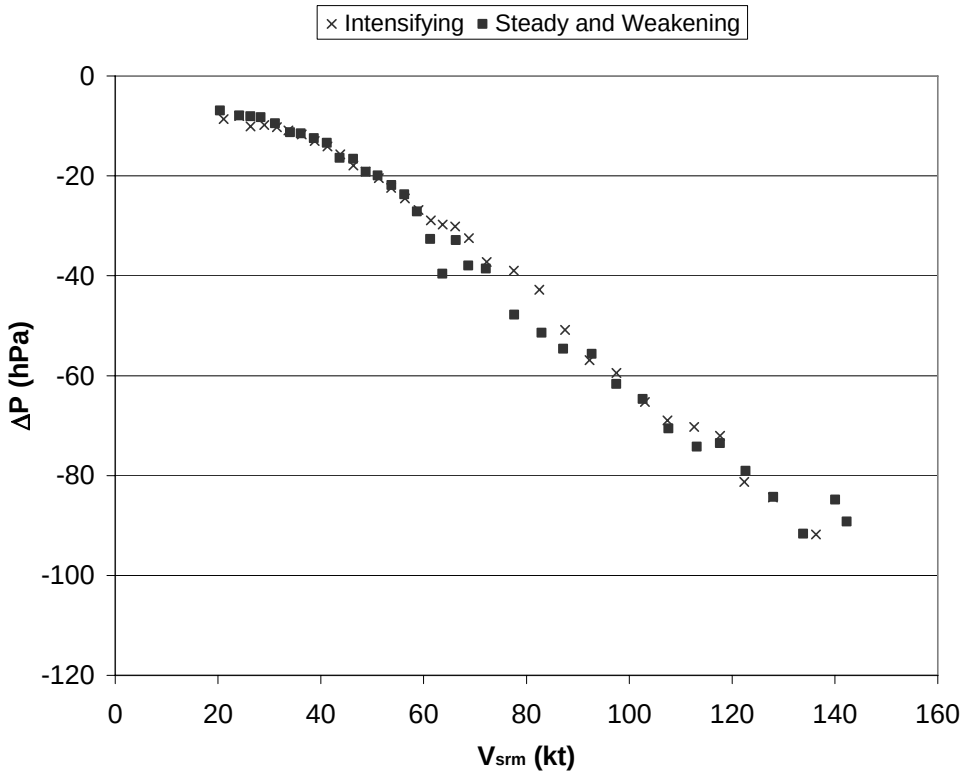

Figure 10. Plots of ΔP vs. V_{srm} for the two intensity trend-based composites.

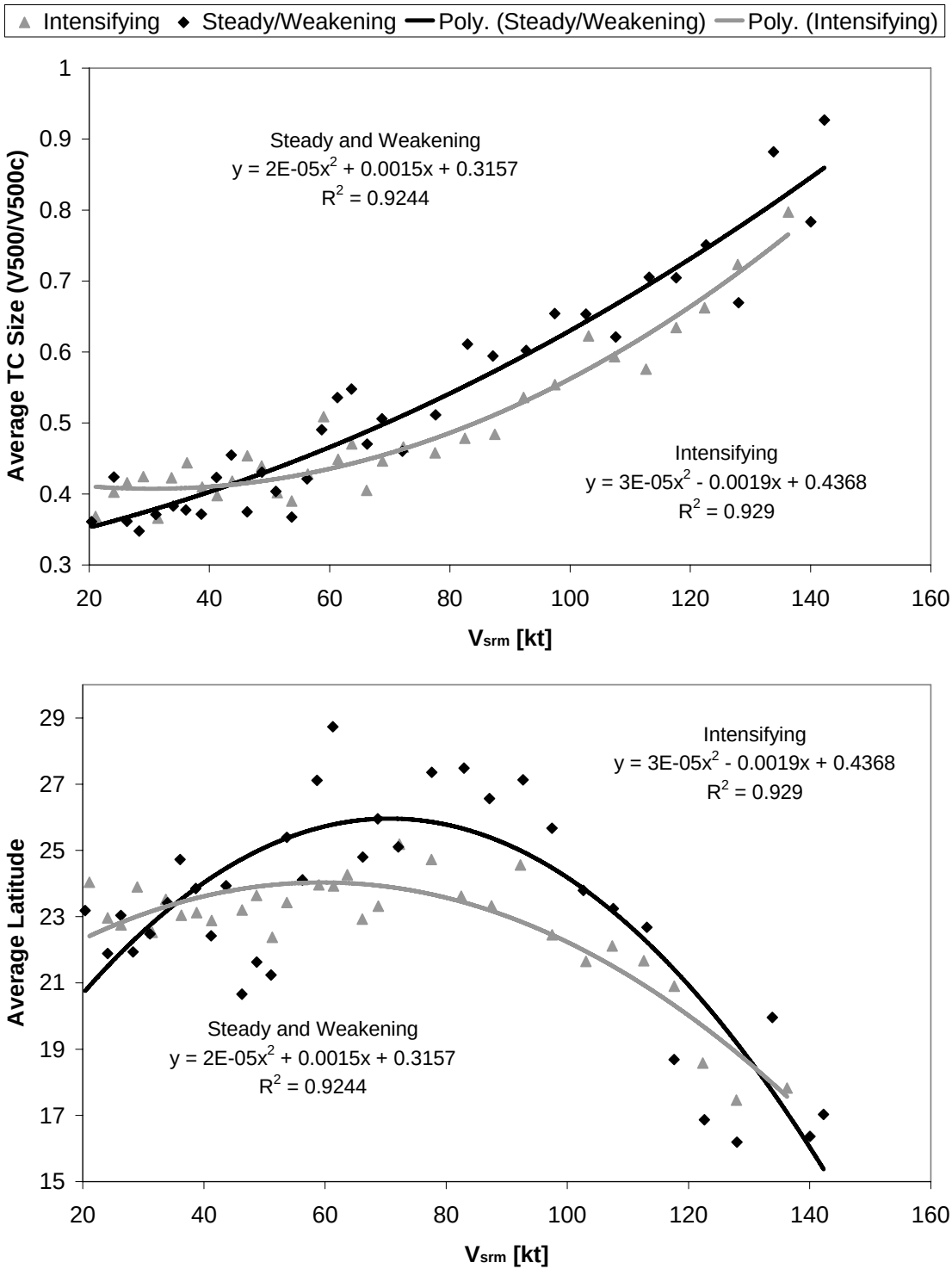

Figure 11. Composite average storm relative maximum surface winds (V_{srm}) versus composite average tropical cyclone size (top) and average tropical cyclone latitude (bottom) are shown. Composites are stratified by 12-h intensity trends. The averages of storms with steady or weakening (intensifying) intensity trends are shown by the black (grey) points. Second order polynomial trend lines are added with the same shading.

a.

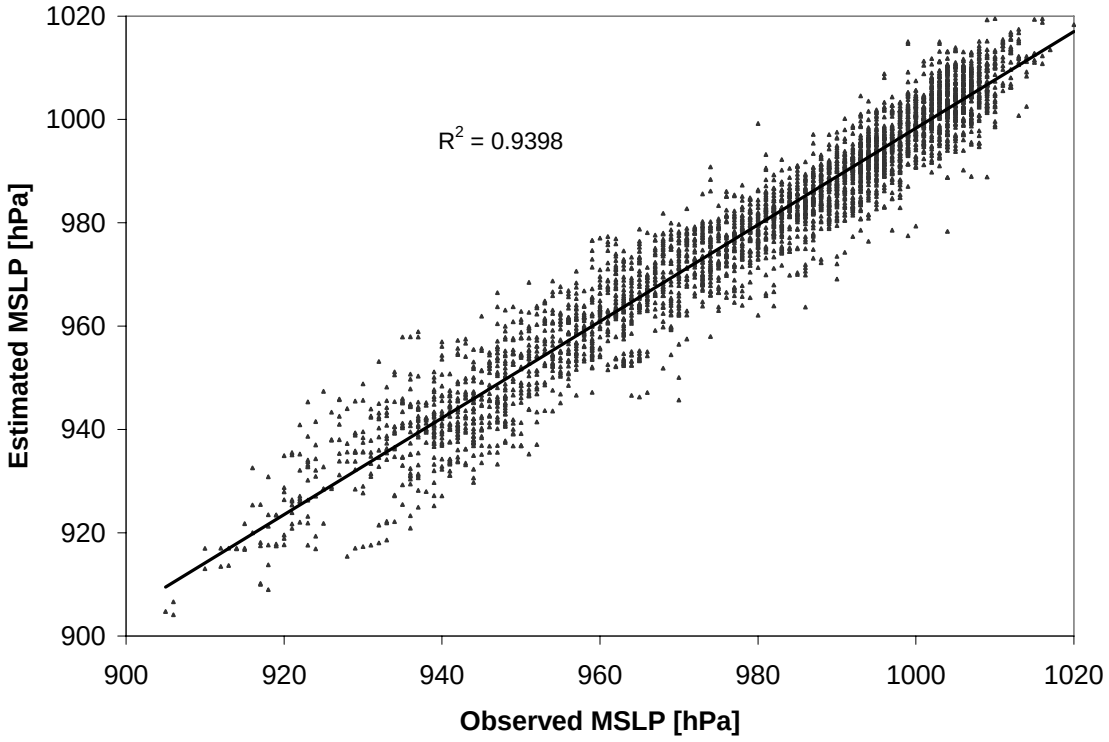

b.

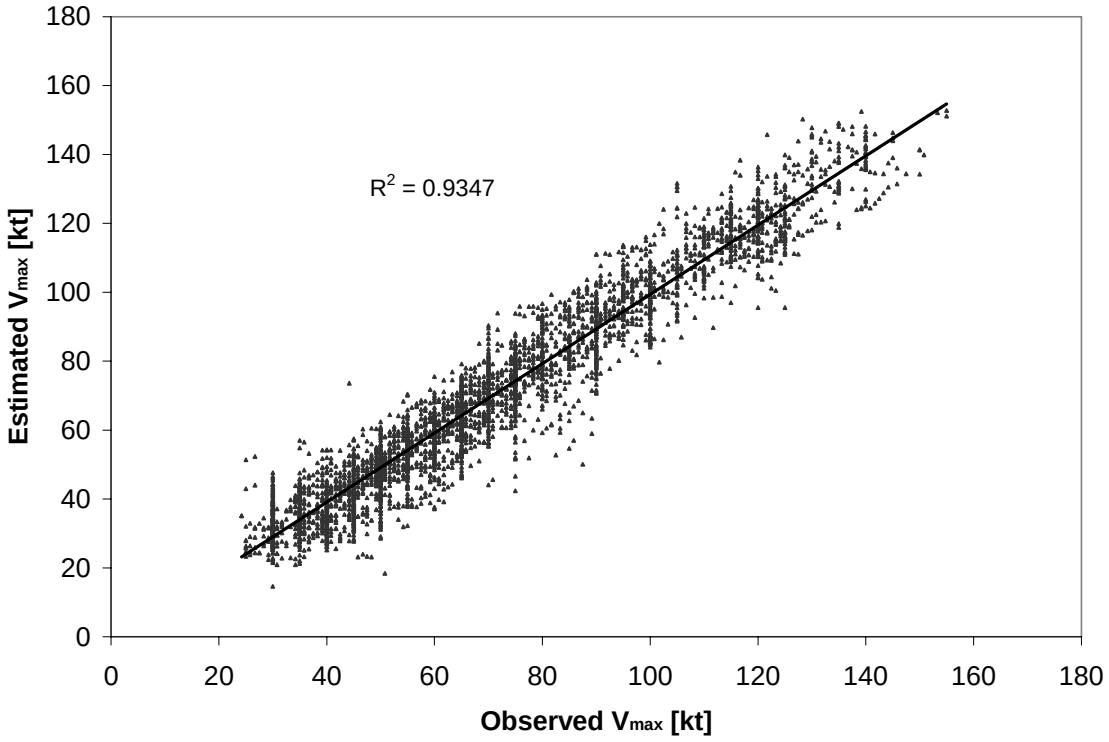

Figure 12. Show the dependent results of Eq. 7 for predicting MSLP given V_{max} (a) and Eq. 8 for estimating V_{max} given MSLP (b).

a.

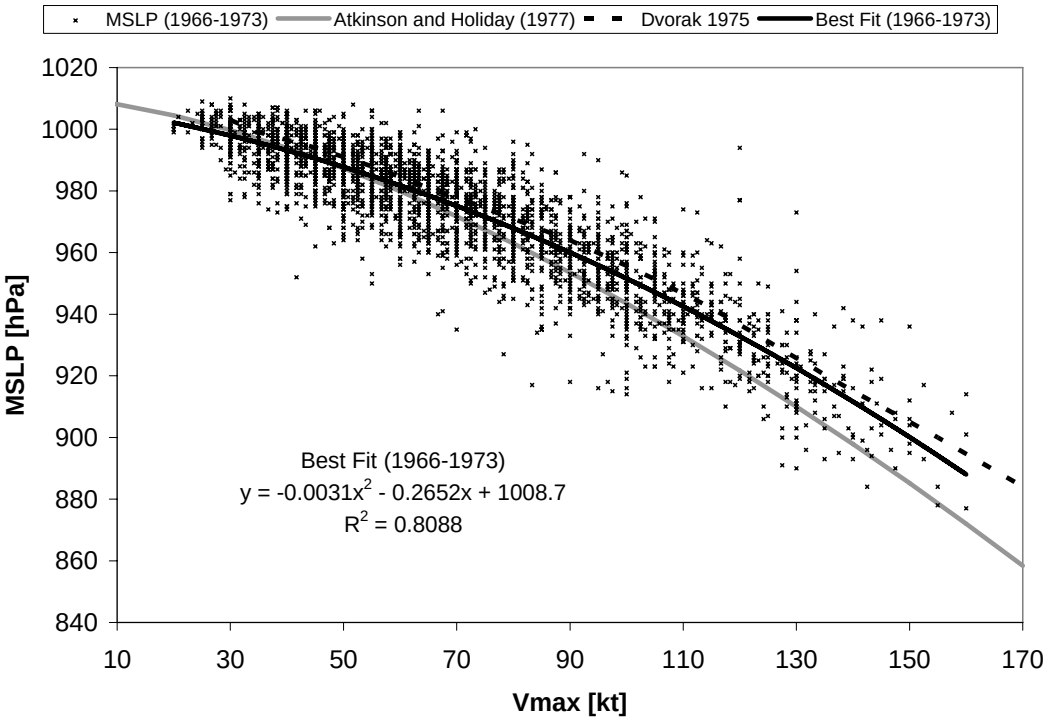

b.

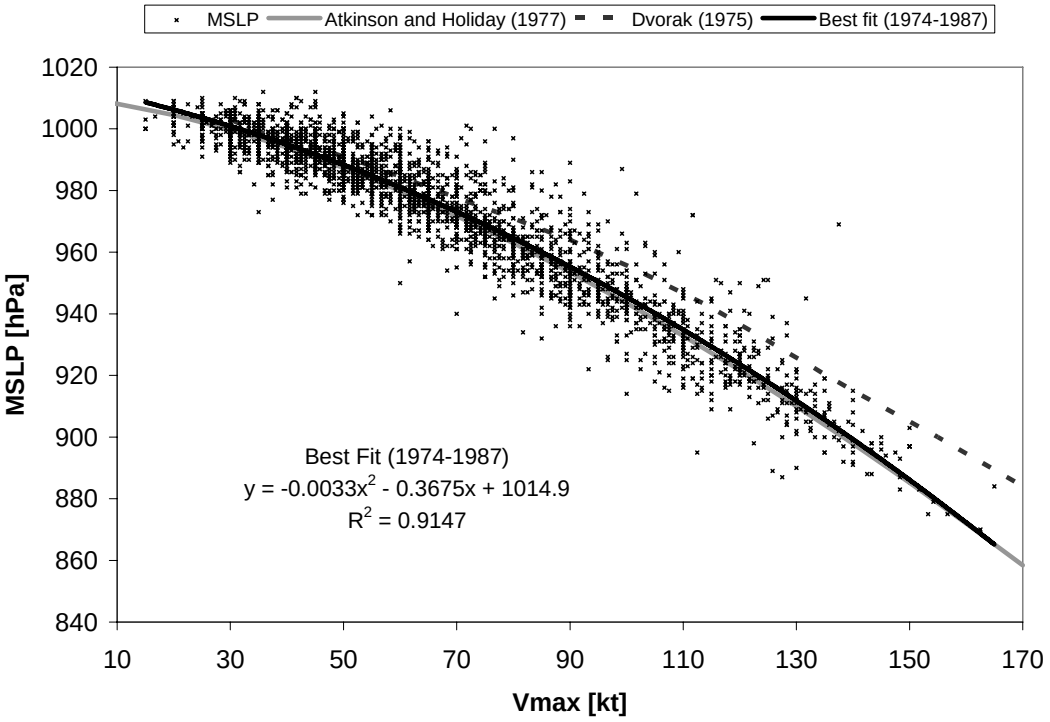

Figure 13: MSLP vs best track maximum surface winds (Vmax) interpolated to the time of the observations and associated best fit relationships to these data for 1966 -1973 (a) and 1974-1987 (b). Also shown are the A&H and Dvorak (1975) WPRs.

a.

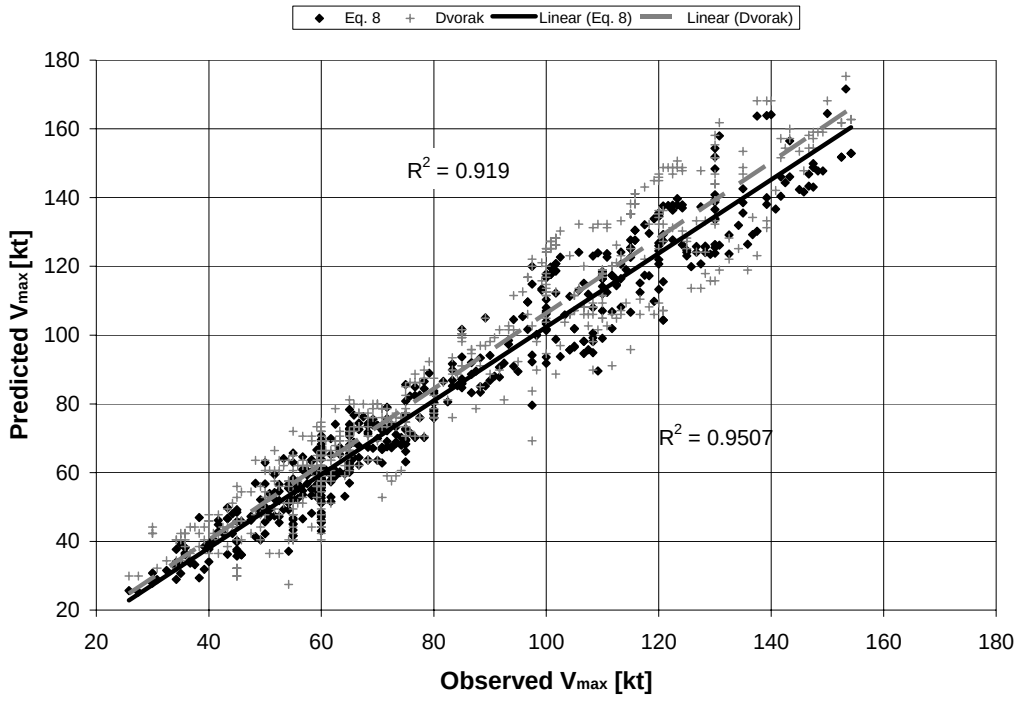

b.

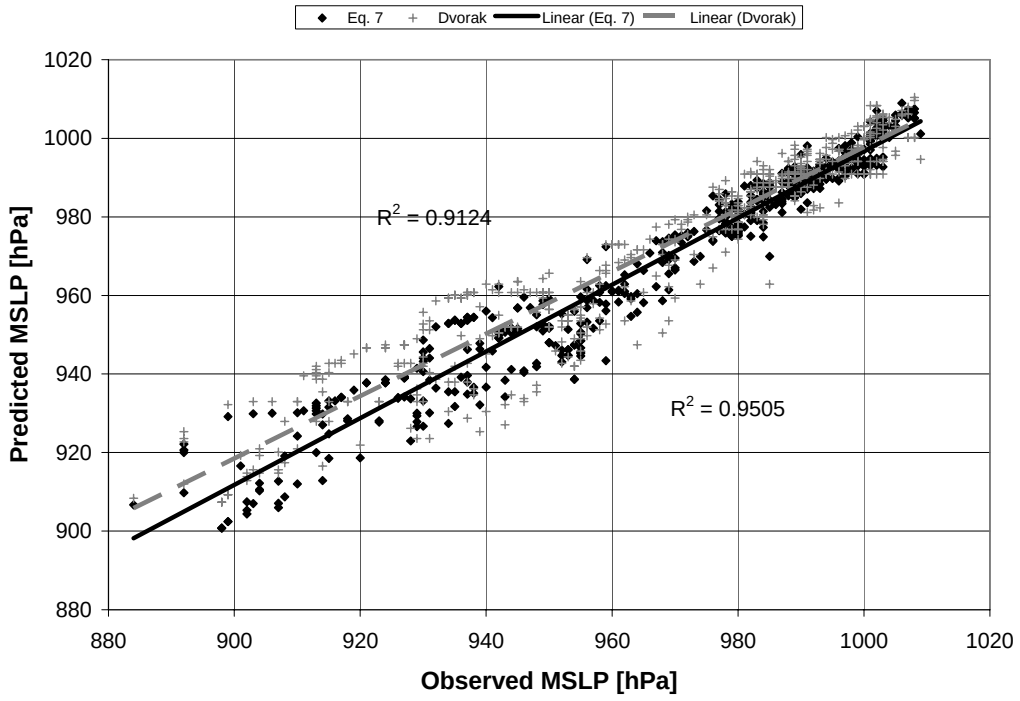

Figure 14: Scatter diagram of the independent predicted values of V_{max} using equation 8 (black boxes) and the Dvorak WPR (crosses) vs. observed values of MSLP from the operational best track (top). A similar scatter diagram for Eq.7 (black boxes) and the Dvorak WPR (crosses) vs. observed MSLP (bottom). Best linear fits for Eq.8 and Eq. 7

are shown with a solid black line in each repective panel with the associated variance explained at the bottom right. Best linear fits for the Dvorak WPR are shown by the gray dashed lines with the associated variance explained in the upper left. Sample includes 534 cases.

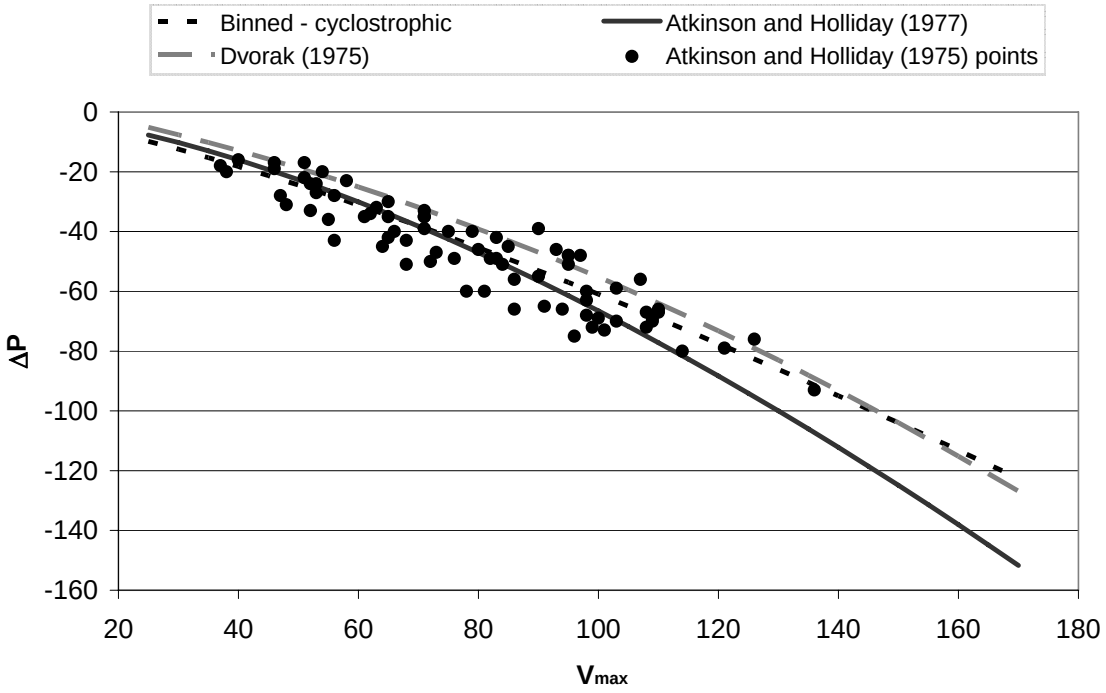

Figure A1: Various wind-pressure relationships plotted along with the Atkinson and Holliday (1977; 1975) developmental data. Shown are the A&H(1977), a fit to the binned raw data assuming a cyclostrophic form, and the Dvorak (1975) WPR. To plot these curves in terms of DP 1010 hPa is assumed to be the environmental reference pressure.

Table 1. Mean Statistics of the individual composites.

Sample	Number	Average Latitude	Average Size	Average V_{max}	Average V_{max} Trend	Average P_{env}	Average Speed [kt]	Average MSLP
Whole	3801	23.67	0.49	72.15	2.55	1014.25	9.61	979.61
<20^o	1226	16.51	0.48	74.86	1.99	1013.18	10.00	979.45
20^o – 30 ^{o}	1917	24.94	0.48	71.30	3.42	1014.27	9.07	979.74
> 30 ^{o}	659	33.33	0.52	69.57	1.04	1015.18	10.44	979.52
Small	595	23.43	0.18	59.16	2.44	1015.12	9.81	992.74
Average	2562	23.43	0.47	69.70	3.03	1014.18	9.68	982.03
Large	644	24.88	0.83	93.90	0.71	1013.72	9.14	957.84
Steady and Weakening	1746	24.27	0.51	73.16	-5.66	1014.48	9.60	977.97
Intensifying	2056	23.17	0.47	71.30	9.52	1014.06	9.62	980.99

Table 2. Statistics associated with the Eq. 7 using the observed environmental pressure(P_{env}), Eq. 16 using the climatological environmental pressure (P_{clim}) from the sample, the Atlantic Dvorak, Koba et al (1990), A&H, Love and Murphy (1985) and Crane WPRs. Bias and error statistics that are statistically different than those produced by Equation 7 are shown as italicized and gray and italicized and boldface for the 95%, and 99% levels, respectively.

	Eq 7 P_{env}	**Eq. 7 P_{cli}**	**Dvorak Atlantic**	**Koba et al. (1990)**	**Atkinson and Holliday (1977)**	**Love and Murphy (1985)**	**Crane**
Bias	-0.5	-0.5	*0.9*	***-7.0***	***-8.2***	-1.2	***-7.9***
RMSE	5.8	6.3	*7.1*	***9.9***	***11.5***	***8.1***	***10.6***
MAE	4.4	4.8	*5.4*	***8.2***	***9.1***	***6.4***	***8.8***

Table 3. Statistics (R^2, bias, RMSE and MAE) associated with the Eq. 8 using the observed environmental pressure(P_{env}), Eq. 8 using the climatological environmental pressure (P_{clim}) from each regional sub sample along with the appropriate Landsea et al. (2004) regional WPRs utilizing a reference pressure equal to 1013 and of Penv . Bias and error statistics that are statistically different than those produced by Equation 8 are shown as italicized and gray and italicized and boldface for the 95%, and 99% levels, respectively.

South of 25N N=1540, df=85

	Eq. 8 using P_{env}	**Eq. 8 using P_{cli}=1013.6**	**Landsea et al., P_{ref}=1013**	**Landsea et al P_{ref}= P_{env}**
R^2	0.95	0.93	0.92	0.94
Bias	-.1.04	-1.29	***-2.32***	-1.13
RMSE	7.67	*8.68*	***9.54***	8.04
MAE	5.89	*6.55*	***7.29***	6.20

Gulf of Mexico N=818, df=45

	Eq. 8 using P_{env}	**Eq. 8 using P_{cli}=1013.5**	**Landsea et al., P_{ref}=1013**	**Landsea et al P_{ref}= P_{env}**
R^2	0.93	0.92	0.89	0.91
Bias	-0.94	-1.13	***1.78***	***2.88***
RMSE	7.34	8.05	*9.16*	8.34
MAE	5.53	6.10	***7.22***	*6.72*

25N – 35N N=1011, df =56

	Eq. 8 using P_{env}	Eq. 8 using P_{cli}=1015.8	Landsea et al., P_{ref}=1013	Landsea et al P_{ref}= P_{env}
R^2	0.93	0.93	0.90	0.91
Bias	-1.25	-1.50	***1.95***	***6.25***
RMSE	7.64	*8.87*	***9.81***	***10.03***
MAE	6.01	6.75	***7.65***	***8.34***

North of 35N N=165,df=9

	Eq. 8 using P_{env}	Eq. 8 using P_{cli}=1016.3	Landsea et al., P_{ref}=1013	Landsea et al P_{ref}= P_{env}
R^2	0.83	0.79	0.60	0.46
Bias	0.14	0.09	***4.85***	***8.21***
RMSE	7.71	8.93	10.18	*11.73*

MAE	6.27	7.15	*8.74*	*9.68*

Table 4. Independent comparison of results obtained from Eq. 7 and Eq. 8 vs. the operational Dvorak Tables. Data includes 491 fixes from 12 Atlantic tropical cyclones and 1 East Pacific tropical cyclone during the 2005 season. Bias and error statistics that are statistically different are shown as italicized and gray and italicized and boldface for the 95%, and 99% levels, respectively.

Independent Comparison, N=524, df= 29

	Eq. 7 for ΔP	**Dvorak ΔP**	**Eq. 8 for V_{max}**	**Dvorak V_{max}**
R^2	0.95	0.91	0.95	0.92
Bias	***1.55***	***4.43***	***1.14***	***4.69***
RMSE	***7.50***	***10.58***	***6.13***	***11.55***
MAE	***5.30***	***7.67***	***5.06***	***9.02***

Table A1. Biases and MAE associated with the various fits to the raw Atkinson and Holliday (1975) dataset. Listed here are the published A&H WPR (1), the cyclostrophic form fit to the binned A&H data (2), the gradient fit for the binned A&H data (3) and for comparison the gradient fit to the Koba et al. (1990) WPR (4).

	(1) Atkinson and Holliday (1977)	**(2) Cyclostropic fit to binned data**	**(3) Gradient fit to binned data**	**(4) Koba et al. (1990)**
MAE	6.64	5.88	5.80	5.80
BIAS	-0.69	1.64	0.36	0.77

Table B1. Dvorak CI vs ΔP tables for storms occurring equatorward of 20^{o} latitude.

Equatorward of 20^{o}

	Small	Average	Large
CI	**ΔP**	**ΔP**	**ΔP**
1.5	-2	-4	-8
2.0	-4	-7	-11
2.5	-7	-10	-14
3.0	-13	-16	-20
3.5	-20	-22	-27
4.0	-27	-29	-34
4.5	-35	-38	-42
5.0	-45	-48	-52
5.5	-55	-58	-62
6.0	-66	-69	-73
6.5	-76	-79	-84
7.0	-88	-92	-96
7.5	-103	-106	-111
8.0	-118	-122	-126

Table B2. Dvorak CI vs ΔP tables for storms occurring equatorward of 20^o to 30^o latitude.

20^o -30^o

	Small	Average	Large
CI	**ΔP**	**ΔP**	**ΔP**
1.5	-4	-8	-12
2.0	-7	-11	-15
2.5	-10	-14	-18
3.0	-16	-20	-24
3.5	-23	-26	-31
4.0	-30	-33	-38
4.5	-38	-42	-47
5.0	-48	-52	-56
5.5	-58	-62	-66
6.0	-69	-73	-77
6.5	-80	-83	-88
7.0	-92	-96	-100
7.5	-107	-110	-115
8.0	-122	-126	-130

Table B3. Dvorak CI vs ΔP tables for storms occurring poleward of 30^{o} latitude.

Poleward of 30^{o}			
	Small	**Average**	**Large**
CI	**ΔP**	**ΔP**	**ΔP**
1.5	-8	-12	-16
2.0	-11	-15	-19
2.5	-14	-18	-22
3.0	-20	-24	-28
3.5	-27	-30	-35
4.0	-33	-37	-42
4.5	-42	-46	-50
5.0	-52	-56	-60
5.5	-62	-66	-70
6.0	-73	-77	-81
6.5	-84	-87	-92
7.0			
7.5			
8.0			